ETH*zürich*

Seasonal temperature dependency of aquatic branched glycerol dialkyl glycerol tetraethers: A mesocosm approach

Seasonal temperature dependency of aquatic branched glycerol dialkyl glycerol tetraethers: A mesocosm approach

Fatemeh Ajallooeian [a,*], Longhui Deng [b], Mark Alexander Lever [b,c], Cindy De Jonge [a]

[a] *Geological Institute, Earth Science Department, ETH Zurich, Sonnegstrasse 5, 8092 Zurich, Switzerland*
[b] *Institute of Biogeochemistry and Pollutant Dynamics, ETH Zurich, Universtitatstrasse 16, 8092 Zürich, Switzerland*
[c] *Marine Science Institute, University of Texas at Austin, Port Aransas, TX, USA*

ABSTRACT

BrGDGTs, membrane-spanning lipids produced by bacteria, are at the basis of the MBT'$_{5ME}$, a biomarker ratio that has been used as a paleotemperature proxy. However, the response of the MBT'$_{5ME}$ to temperature changes, particularly in freshwater systems, remains incompletely understood. In this study, oxic mesocosms are used to assess the temperature sensitivity of brGDGTs and their producers, sampled from a lake (Lake Rot) and a river (Sihl River) in three different seasons. Three temperature treatments are employed (10, 17.5, and 25 °C), representing control (in-situ temperatures), cooling, and/or warming treatments, with GDGTs and the bacterial community measured at several timepoints (24 h, 1, 2, 3 and 5 weeks). The control experiments showed that this experimental approach could not replicate natural conditions exactly, with small changes in chemistry (pH, conductivity, alkalinity) and bacterial community composition. Still, our mesocosm setup yielded valuable insights into the temperature-dependent production of lacustrine brGDGTs and MBT'$_{5ME}$ values, especially in warming treatments, while no response was observed in cooling treatments, potentially indicating limited sensitivity to cold temperatures. In the river mesocosms not the MBT'$_{5ME}$ but the IR ratio showed a temperature dependency, potentially driven by small changes in the water pH. Coeval changes in the composition of the bacterial community and the MBT'$_{5ME}$ and IR are determined to constrain potential GDGT producers. Although an increase in MBT'$_{5ME}$ in response to some warming incubations is observed, the temperature-sensitivity of MBT'$_{5ME}$, as expected from GDGT studies on a global scale, is not supported by this experiment.

1. Introduction

Quantitative continental temperature proxies, based on geological and biological indicators measured in ice cores, tree rings, sediment cores, or other environmental records are used to reconstruct past climatic conditions. These paleoclimate reconstructions are used to improve climate model predictions (Harning et al., 2020; Tierney et al., 2020). Providing more accurate values that allow for quantitative analyses of past temperature variations aids in understanding the mechanism, magnitude, and frequency of past climate change (Marcott and Shakun, 2015).

A group of bacterial membrane spanning lipids, so-called branched glycerol dialkyl glycerol tetraethers (brGDGTs), have been used as paleotemperature (mean annual temperature: MAT) indicators (Weijers et al., 2007; Peterse et al., 2009; Tierney and Russell, 2009) in geological archives such as paleosoils, marine and lake sediments (Xiao et al., 2016;

Russell et al., 2018; Zang et al., 2018). These lipid molecules contain two glycerol backbones that are attached to two branched alkyl chains with four ether bonds (Sinninghe Damsté et al., 2000; Weijers et al., 2006). Their structural variability (Supp. Fig. 1) is caused by a change in the degree of methylation (containing 4 to 6 branches, so-called tetra, penta and hexamethylated brGDGTs) and by the presence of 1 or 2 cyclopentyl moieties formed by internal cyclization (Schouten et al., 2013). Compounds with the outer branch(es) located on the C-α and/or ω5 are denoted as 5-methyl, brGDGTs, whereas compounds with the outer methyl branch(es) on C-α and/or ω6 are referred to as 6-methyl brGDGTs (De Jonge et al., 2013).

As brGDGT compounds are generally abundant in soils (Schouten et al., 2000), their presence in marine and lacustrine sediments was initially assumed to indicate the presence of soil organic matter. However, it has since been confirmed that brGDGTs measured in the lacustrine water column and sediments are dominantly produced within the

---

water column of lakes and rivers (De Jonge et al., 2014a; Loomis et al., 2014; Martínez-Sosa and Tierney, 2019; Martínez-Sosa et al., 2020) or within surface sediments (Buckles et al., 2014). On a global scale, the degree of methylation of 5-methyl brGDGTs (calculated as the MBT'$_{5ME}$ ratio) correlates with temperature (Martínez-Sosa et al., 2021) in lacustrine settings. Similarly, the cyclization index of tetraethers (CBT' ratio), which expresses the relative abundance of cyclopentane-containing tetramethylated brGDGT Ic and 6-methyl penta- and hex-amethylated brGDGTs compared to their 5-methyl counterparts without cyclopentane group, correlates with lake pH (Raberg et al., 2021). The isomer ratio (IR, De Jonge et al., 2014b; Halffman et al., 2022), which expresses the relative abundance of 6-methyl penta- and hexamethy-lated brGDGTs compared to their 5-methyl counterparts, reflects vari-ation in similar pH-sensitive compounds as the CBT' ratio. As such, IR values have also been linked to both pH and conductivity (Russell et al., 2018; Martínez-Sosa et al., 2020; Raberg et al., 2021), but also with temperature (Martínez-Sosa et al., 2020). To translate variation in MBT'$_{5ME}$ values and mean annual temperature (MAT), or temperature above freezing, several lacustrine calibrations have been developed (e. g., Russell et al., 2018; Martínez-Sosa et al., 2021; Raberg et al., 2021). These calibration between the MBT'$_{5ME}$ ratio and MAT have been based on empirical dependencies, either among global or local temperature gradients (e.g., Russell et al., 2018, Stefanescu et al., 2021).

More recently, these empirical calibrations have been underpinned by mechanistic understanding of the temperature-dependency of the MBT'$_{5ME}$ ratio. Using computer simulations, Naafs et al. (2021) corroborate the notion that bacterial membrane lipids change directly with temperature, a process referred to as homeoviscous adaptation. This is supported by temperature-dependent adjustments in the composition of GDGT lipids of specific bacterial cultures (*S. usitatus*) (Chen et al., 2022; Halamka et al., 2022). These studies support the idea that the empirical calibration of MBT'$_{5ME}$ relies on the homeoviscous adaptation of a potentially limited diversity of bacteria.

However, previous studies have employed simultaneous analysis of GDGT lipids and 16S rDNA based community composition to propose that brGDGT distributions change as the communities of bacterial brGDGT producers change in the environment (e.g. Weber et al., 2018; De Jonge et al., 2019; 2021; Guo et al., 2022). As the phylogenetically diverse phylum Acidobacteria is a potentially important source for brGDGTs in soils (Weijers et al., 2009), acidobacterial cultures from different subgroups have been the subject of lipid profiling. Here, Sin-ninghe Damsté et al., (2011, 2014, 2018) report the presence of distinct ether and ester-bound *iso*-diabolic acids and branched fatty acids that are possible precursors of brGDGT lipids, in subgroups 1, 3, 4 and 6. In soil environments, shifts between Acidobacterial subgroups are observed when 6-methyl GDGTs or brGDGT Ia are produced in non-arid soils (De Jonge et al., 2019; 2021), while Verrucomicrobiae (Sparto-bacteria) are potential producers in arid soils (Guo et al., 2022). The substantial production of brGDGTs contrasts with the low abundances of Acidobacteria in lake water columns (Dedysh and Sinninghe Damsté, 2018; Weber et al., 2018; van Bree et al., 2020), and raises the question whether additional groups are involved in brGDGT synthesis in aquatic settings. Moreover, genomic analyses show the widespread potential among bacterial phyla to produce membrane-spanning lipids that contain ether bonds (Sahonero-Canavesi et al., 2022; Zeng et al., 2022).

Although changes in bacterial community composition across freshwater redox gradients (e.g., the oxic, suboxic water columns) are coeval with changes in brGDGT signature and MBT'$_{5ME}$ values and bacterial community composition (Weber et al., 2018), the impact of temperature on lacustrine brGDGT producers is still poorly constrained. Charactering the temperature response of brGDGT lipids, together with potential bacterial brGDGT producers allows study of whether homeo-viscous adaption or changes in the bacterial community drive temperature-dependent brGDGT variation in freshwater systems.

Understanding these drivers behind brGDGT variations in freshwater systems is especially important as these settings experience seasonal

changes. To determine the temperature response of brGDGTs, their distributions have been tracked over different seasons within individual lakes (Loomis et al., 2014; Miller et al., 2018). However, because other variables, such as water chemistry and bacterial community also un-dergo seasonal changes (Shade et al., 2007), a laboratory approach is needed to study the unique impact of temperature on GDGTs as done by Martínez-Sosa et al., (2020) using mesocosms. We build both upon this experimental approach and the knowledge on confounding factors on empirical calibrations. A mesocosm approach will allow experimental change (specifically, temperature), while measuring proposed con-founding variables such as water chemistry (pH, alkalinity, conductiv-ity), and allow monitoring of both production of brGDGTs and their bacterial producers. Here we experimentally assess the following hy-potheses: (H1) use of oxic mesocosms consistently allows to replicate natural freshwater systems and brGDGT production (H2) the same temperature dependency of MBT'$_{5ME}$ is observed in local freshwater settings (both in situ and after incubation) as at the global scale, (H3) temperature changes have a stronger impact on brGDGT compositions than changes in water chemistry and (H4) changes in the MBT'$_{5ME}$ and IR are coeval with changes in the bacterial community composition. Examining the temperature sensitivity of brGDGTs in freshwater sys-tems using an experimental approach can enhance the proxy's reliability for past temperature calibrations.

2. Materials and methods

2.1. Sampling sites and seasons

Two sites, a freshwater lake and a river, are each sampled in 3 different seasons. Water was collected from the oxic surface of Lake Rot (Rotsee, 47°04′10.1″N; 8°18′48.1″E) and Sihl River (47°21′05.8″N; 8°31′12.7″E), from the lake shore and riverbank, on a seasonal basis in April-May, July-August, and October-November 2021. With a surface area of 0.48 km² and depth of 16 m, eutrophic Lake Rot (Smith et al., 1999; Su et al., 2017) experiences seasonal stratification and the development of an anoxic bottom layer every summer because of the high aerobic mineralization rates of phytoplankton-derived organic matter (Schubert et al., 2010; Naeher et al., 2014). Brook Ron, a small artificial subsidiary of the Reuss River, is the single inlet flowing into Lake Rot. Sihl River has a total length of 73 km with a headwater located at 1650 m altitude (Druesberg mountain), including the Sihlsee reser-voir at 41 km upstream of the sampling point. As a subalpine river, the Sihl is mainly characterized by a steep morphology, high turbidity, and dynamic waterflow throughout the year (Schwab et al., 2022). For this experiment, water was collected from a downstream location with less turbidity.

2.2. Experimental design

For each starting condition (n = 6, three seasons and two sites), 2 L of freshwater are filtered on site to record brGDGT of in situ conditions (T0). Afterwards, water canisters (360 L in total) were transported back to the Swiss Federal Institute of Technology (ETH Zurich), Geological Institute. Here, the water was divided into 2 L mesocosm bottles (n = 30 for each starting condition, Fig. 1). The bottles were placed on stirring plates (v = 100 rpm) to ensure water mixing and covered with perfo-rated plastic caps to allow circulation of air. The bottles ("Mesocosms") were set up in a temperature-controlled climate chamber, where the natural day/night cycles were mimicked (both light intensity and duration of the day-night cycle mimicked seasonal condition (e.g., spring mesocosms were set up with light intensity and daylight hours similar to spring in Switzerland). They were subjected to 3 different temperature treatments, that were selected based on 24-hour averages of sampling dates during the past 5 years to reflect realistic in situ temperatures at the 3 seasons under study (10 °C, 17.5 °C and 25 °C, for spring, autumn, and summer, respectively, Fig. 1). Mesocosm bottles
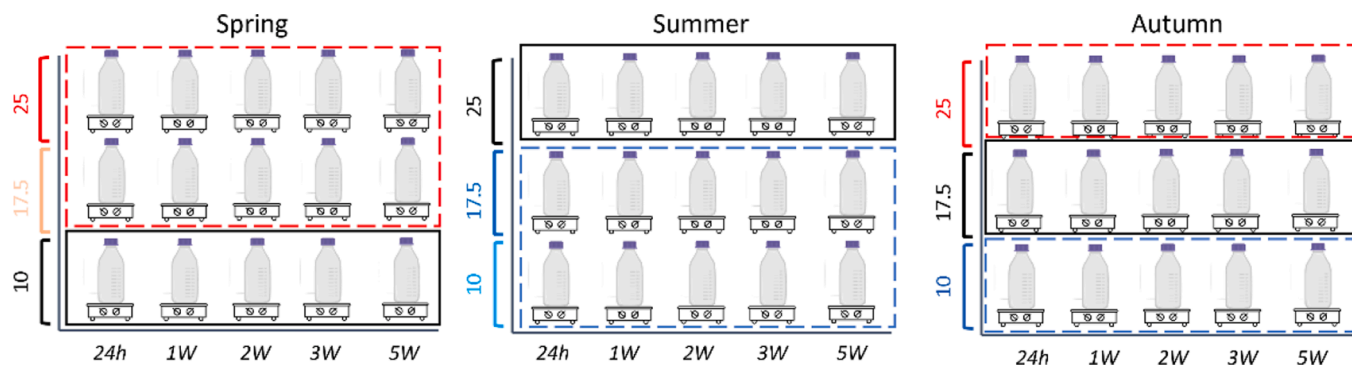
Fig. 1. A diagram illustrating the seasonal mesocosm setup. The control mesocosms for spring, summer, and autumn are maintained at in-situ temperatures of 10 °C, 17.5 °C, and 25 °C, respectively marked by black boxes around the mesocosms. Spring mesocosms are subjected to two warming treatments (17.5 °C and 25 °C) marked by dashed red boxes, while summer mesocosms are subjected to two cooling treatments (10 °C and 17.5 °C) marked by dashed blue boxes. In the case of autumn incubations, both a cooling (10 °C, blue series) and warming (25 °C, red series) treatments are employed. (For interpretation of the references to color in this figure legend, the reader is referred to the web version of this article.)

were thus subjected either to constant temperatures comparable to temperatures at the time of sampling ('control treatment'), increased temperatures ('warming treatments') or colder temperatures ('cooling treatments'). Specifically, for spring, where T0 water temperature was 10 °C and 11.1 °C in Lake Rot (LR) and Sihl River (SR), respectively, 10 mesocosm bottles received a control treatment (10 °C), while two sets of 10 bottles were subjected to two separate warming treatments (17.5 °C and 25 °C). For autumn waters (in situ water temperatures LR = 15.5 °C, SR = 18 °C), mesocosm bottles were subjected either to a control treatment (17.5 °C), a warming treatment (25 °C) or a cooling treatment (10 °C). In summer, the 25 °C represented the control treatment (T0 water temperatures at LR:22.5 °C, SR:23 °C), while two sets of mesocosm bottles were subjected to cooling treatments (at 10 °C and 17.5 °C). The range of temperatures was thus realistic, although the rate of temperature change (sudden warming or cooling) did not mimic natural conditions. To capture the response of brGDGTs and their bacterial producers to these individual temperature treatments with time, the two entire 2 L mesocosms were sacrificed and filtered at 5 timepoints (24 hrs, 1 week, 2 weeks, 3 weeks, and 5 weeks (T1 toT5, respectively). The timepoints were selected using previous information on approximate growth/decay times of brGDGTs, with maximum brGDGT concentrations observed after 1–2 weeks, and a gradual decrease in concentration thereafter (Martínez-Sosa and Tierney, 2019). For each timepoint, the water chemistry and GDGT distribution of two independent mesocosms were analysed as duplicates, to determine variability. Due to an extraction preparation error, the Sihl River autumn mesocosms reports are based on 1 set of bottles (no duplicates).

2.3. Sampling and characterization of brGDGT lipids, water chemistry and bacterial DNA

2.3.1. Sampling

The mesocosms of each temperature treatment were filtered over 0.22 μm PVDF membrane filters (Durapore®, Germany) placed on a titanium tripod (cleaned using ethanol (EtOH), methanol (MeOH), and dichloromethane (DCM) between samples). PVDF filters allow collection of brGDGT lipids with high efficiency (Martínez-Sosa and Tierney, 2019) at their respective timepoints. Following filtration, a fixed area of the PVDF filter (16 mm^2) for bacterial community analysis was preserved and stored at −20 °C for later analysis, the remaining filter was dissected and subjected to lipid biomarker extraction.

2.3.2. Lipid extraction

Lipid extraction was performed by acid hydrolysis of the filters, where the freeze-dried filters were placed in centrifuge tubes and 10 mL of 1.5 N HCl (HCl/MeOH 1:7 (v:v)) was added. Tubes were capped and

wrapped with Teflon tape and heated at 80 °C for 2 h. This process allows the conversion of all intact polar lipids (IPL) into core lipid (CL) brGDGTs to maximize the recovery of all brGDGT compounds (Weber et al., 2017). Afterwards, DCM was added to samples to obtain a MeOH/DCM 1:1 (v:v) solvent composition and allow phase separation. Subsequently, the samples were extracted with DCM three times. The total lipid extract (TLE) was subjected to column chromatography using a 3.4 cm column packed with aluminium oxide (alox), using 3 solvent mixtures, hexane/DCM 9:1 (v:v), hexane/DCM 1:1 and MeOH/DCM 1:1 for the fraction containing GDGTs. After the addition of a known amount of C46 GTGT standard (Huguet et al., 2006), the polar fractions were filtered over a 0.45 μm PTFE filter, dried under N$_2$ and re-dissolved in 50 μL of hexane/isopropanol (IPA) 99:1 (v:v) before analysis using a high-performance liquid chromatography–mass spectrometry (HPLC–MS, Agilent Technologies®-1200, USA) after Hopmans et al., (2016), with modified column temperature (40 °C) and an injection volume of 10 μL. This method allows detection of all 15 brGDGT compounds (Schouten et al., 2007; Hopmans et al., 2016). Ions with known mass over charge ratios (m/z 1050, 1048, 1046, 1036, 1034, 1032, 1022, 1020, 1018) for brGDGTs were detected and semi-quantified according to the internal standard's (m/z 744) peak area corresponding to the added concentration (10 ul = 49.6 ng). The instrumental error was determined to be approximately 15 % of concentrations.

The MBT'$_{5ME}$ (De Jonge et al., 2014b) and the Isomer Ratio (IR) were calculated after De Jonge et al., (2014a), including only compounds without cyclopentane moieties. While IR has been described to vary both with pH in soils (Naafs et al., 2017) and temperature in lakes (Russell et al., 2018; Martínez-Sosa et al., 2021), other indices including CBT' (De Jonge et al., 2014a) and DC' have been proposed to correlate with soil pH (De Jonge et al., 2014b, 2021) and lake water column pH (Russell et al., 2018). The reconstructed water temperature (T$_{rec.}$) was calculated based on both Russell et al. (2018) and Martínez-Sosa et al., (2021) calibrations, although both yielded comparable results. Expressions of indices discussed above are described below:

$$MBT'_{5ME} = \frac{Ia + Ib + Ic}{Ia + Ib + Ic + IIa + IIb + IIc + IIIa}$$

$$IR = \frac{IIa' + IIIa'}{IIa' + IIIa' + IIa + IIIa}$$

$$DC' = \frac{Ib + IIb + IIb'}{Ib + IIb + IIb' + Ia + IIa + IIa'}$$

$$CBT' = log_{10}\frac{(Ic + IIa' + IIb' + IIc' + IIIa' + IIIb' + IIIc')}{Ia + IIa + IIIa}$$

$$MATrec = -1.21 + 32.42 \times MBT'_{5ME} \ (R^2 = 0.92, \text{ p-value} < 0.0001,$$

RMSE = 2.44 °C).

2.3.3. Water chemistry measurements

To characterize changes in the water chemistry through time, at each time point (T0 –T5W) aliquots of each mesocosm were taken for anions (Nitrate - NO_3^-, Sulfate - SO_4^{2-}, Chloride - Cl^-), and cations (Calcium - Ca^{2+}, Sodium - Na^+) (measurements using ion chromatography (compact ion chromatograph pro, Model 88, Metrohm Inc, Switzerland) and alkalinity measurements using an 862 Compact Titrosampler (Metrohm Inc, Switzerland, international standard organization method EN ISO 9963–1:1995)). Furthermore, pH, temperature and conductivity of the samples were measured with a multimeter (MultiLine® IDS 3620, Xylem Inc. USA) at the time of filtration.

2.3.4. DNA extraction, quantitative PCR, and 16S rRNA gene sequencing

A known fraction (16 mm^2) of each filter was cut-up and stored in 2 mL PCR-clean tubes. These samples underwent DNA extraction following the modular protocol of Lever et al. (2015). In short, dNTP solution (10 mM) was added to samples to reduce DNA sorption and allow maximum DNA recovery, followed by the addition of cell lysis solution and incubation of samples on a shaker for 1 h at 50 ℃. Subsequently the DNA containing supernatant was washed twice with a cold 24:1 (v:v) chloroform-isoamyl alcohol mixture. NaCl, Linear Polyacrylamide (LPA) and EtOH were added, and the extracted DNAs were precipitated in room temperature at dark for 2 h. DNA pellets were washed three times with 70 % EtOH to remove excess NaCl and were dried before dissolution in molecular grade water.

The abundance of bacterial 16S rRNA genes were determined by quantitative PCR (qPCR) assay using a LightCycler 480 II (Roche Life Science, Switzerland) (Deng et al., 2020, Han et al., 2020). The 16S bacterial primers BAC908F (5′-AACTCAAAKGAATTGACGGG-3′) and BAC1075R (5′-CACGAGCTGACGACARCC-3′) were mixed with a SYBR Green I-based master mix (0.5 μL of each primer, 5 μL of SYBR Green I (Roche Life Science, Switzerland), 1 μL of H$_2$O, 1 μL of BSA). The 16S Bacteria DNA quantification was performed by comparison with a dilution series of a known DNA concentration. During the qPCR runs, the negative control (molecular grade water) showed average Cp values of 28–30. To ensure accuracy, a Cp cut-off of 27 was selected. Samples exhibiting a higher Cp value (>27) were determined to have too low 16S rRNA contents and excluded from downstream analyses. Instead, bacterial OTUs (Operational Taxonomic Units) identified using samples with Cp > 27 were used as examples of potential contaminant taxa. Sequence libraries were prepared according to a standard workflow (Deng et al., 2020, Han et al., 2020). Briefly, amplicons of bacterial 16S rRNA gene were obtained through PCR reactions using the primer pairs S-D-Bact-0341-b-S-17 (5′-CCTACGGGNGGCWGCAG-3′)/S-D-Bact-0785-a-A-21 (5′-GACTACHVGGGTATCTAATCC-3′). Amplicon sequencing was done via paired sequencing using the Illumina MiSeq platform at the genetic diversity center (GDC) of ETH Zurich. Positive (Plasmids of 16S rRNA genes from *Holophaga foetida* (Acidobacteria)) and negative controls (molecular grade water) were added to ensure the quality of the sequencing run.

Although data loss was not significant during the back-mapping efficiency of the raw sequencing data, the number of high-quality zOTUs (denoised sequencing data) remained high and about 30 % of the sequences could not be mapped to clusters. An abundance threshold of 5 was adopted which resulted in increased mapped sequences with an increased number of zOTUs (n = 7893). Chimera reads were consequently removed, and 5348 non-chimeric OTUs were kept. The USEARCH algorithm with global alignments with the identity threshold of 97% was used to map all the sequencing reads, providing an OTU Table with 3817 taxa and a total of 4,517,711 OTU reads. The total reads were then rarefied to the depth of 5100 reads per sample, retaining 3037 taxa, and total of 117,300 reads in 25 samples. The 16S rRNA genes of all T0 conditions were quantified and sequenced successfully.

2.4. Statistical analysis

A one-way ANOVA was computed to determine significant differences between seasonal brGDGT concentrations at both sites. To determine whether brGDGTs distribution showed variation after the start of the incubation, the MBT'$_{5ME}$ and IR were compared with values measured at T24h (Supp. Table 4). To calculate linear correlations with time, the timepoints (T24h-T5W) are used as time units, and thus not converted into hours. Compounds that are often below the detection limit were excluded from analysis. For Lake Rot this included brGDGTs IIIb, IIIb', IIc', IIIc; no compounds were excluded from the analysis for Sihl River. The correlation between inorganic parameters (pH, alkalinity, conductivity, water ions) and the concentration and fractional abundance of brGDGTs or brGDGT ratios were examined using linear regression methods including the Pearson correlation coefficient (r), and p-value of correlation test between paired samples (where p-values < 0.05 are considered significant). To test whether the composition of the bacterial community in Lake Rot and Sihl River could potentially determine the variation in brGDGT variability between a selected group of mesocosms with distinct MBT'$_{5ME}$ and IR values, a bio-indicator approach is used (De Jonge et al., 2019; Halffman et al., 2022). Here, bio-indicators that are significantly increased in the respective groups (p < 0.1) are reported, with the p-value for this group calculated after Sidak's correction for multiple testing. Downstream and statistical data analysis on brGDGTs and the OTU table were thus performed using packages "phyloseq" (McMurdie and Holmes, 2013) "vegan" (Oksanen et al., 2013), "indicspecies" (De Cáceres, 2013), and "tidyverse" from R v4.1.2.

3. Results

To compare the seasonal variability (T0) with the changes caused by the mesocosm treatments, a comparison between initial (T0) measurements of water chemistry, bacterial community composition, and brGDGTs concentration in Sihl River and Lake Rot is followed by the experimental (mesocosm) results.

3.1. Water chemistry parameters

To ensure that the mesocosm T0 conditions reflect typical freshwater inorganic parameter values, several indicators of the water chemistry in Lake Rot and Sihl River are described.

The inorganic parameters in Lake Rot exhibit similar values in spring and summer, with conductivity of 267 and 249 in spring and summer (μS/cm), pH between 8 and 9, and cations such as Ca^{2+} (1059, 1063 mg/L) and Na^+ (222, 206 mg/L in spring and summer respectively) indicating typical freshwater conditions (Horne and Goldman, 1994; Weyhenmeyer et al., 2019; Rogora et al., 2015). The concentration of SO_4^{2-} in the lake water (<150 mg/L) is similar to other freshwater lakes (Zak et al., 2021), but the concentration of NO_3^- in spring (50 mg/L) slightly exceeds the average freshwater NO_3^- levels, as reported in other studies (>40 mg/L, James et al., 2005). Water alkalinity in Lake Rot is similar to other freshwater lakes in Europe (<100 mg dL^{-1}, Lliros et al., 2014). However, these parameters (pH, alkalinity, conductivity, Na^+, Ca^{2+}, SO_4^{2-}, NO_3^-) decrease during autumn when NO_3^- is below the detection limit (<12 mg/L). In Sihl River, most inorganic parameters exhibit comparable values in spring and summer, that are also similar to Lake Rot. In autumn, some parameters (alkalinity, Na^+, SO_4^{2-}, NO_3^-) increase while pH (8.3) and Ca^{2+} (1430 mg/L) remain stable (Fig. 2). These parameters, nonetheless, remain within the boundaries of standard freshwater river conditions (Bódis et al., 2016). Following the initiation of the incubation period, the minor variability in the mesocosm water chemistry is summarized in Fig. 2. As the impact of the water chemistry parameters pH and conductivity on brGDGT distribution has been observed previously in lacustrine environments (Stefanescu et al., 2021; Wang et al., 2021), changes in the mesocosm water chemistry are
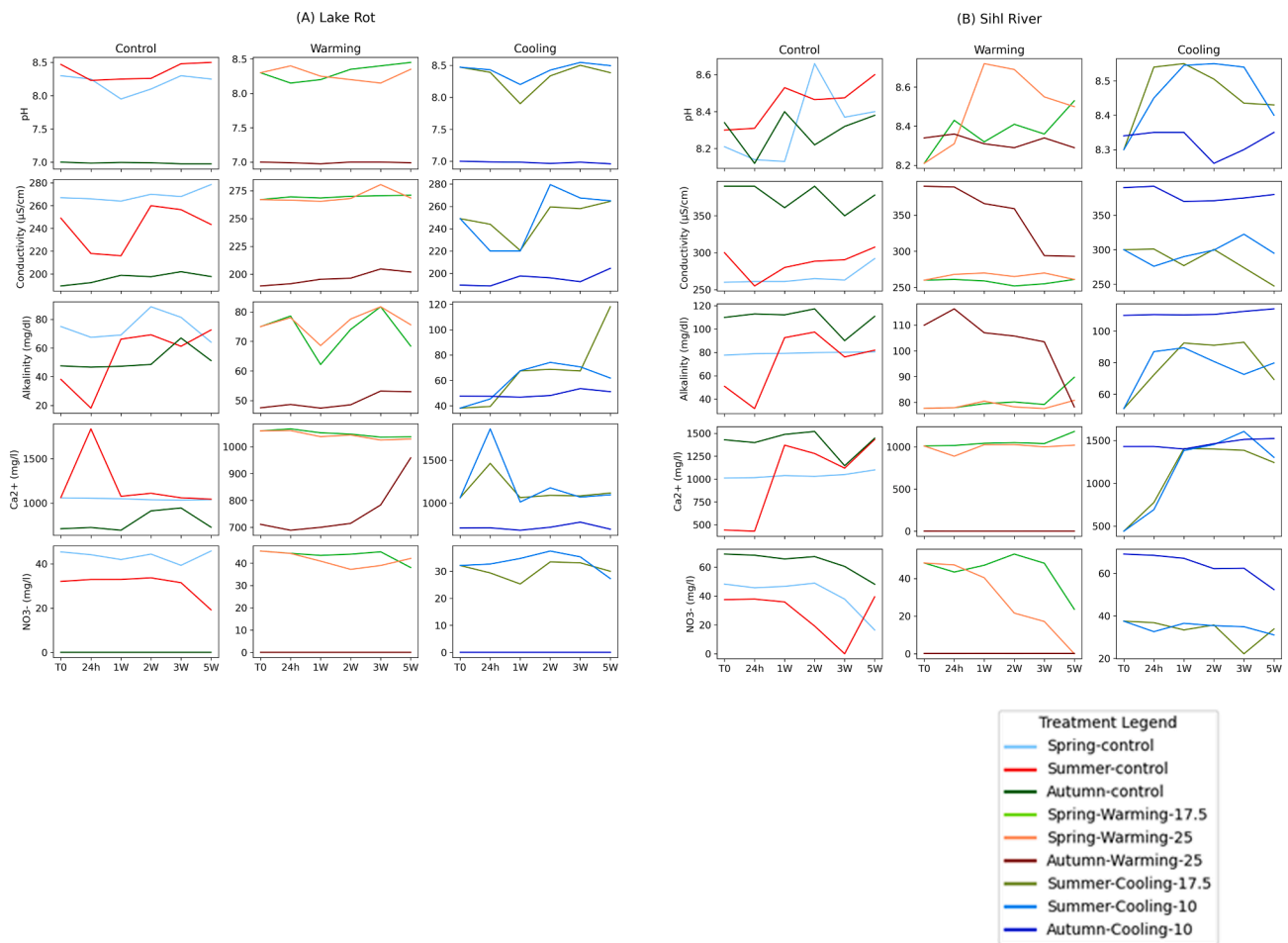
Fig. 2. Line plots representing changes with time of selected water chemistry parameters measured in Lake Rot and Sihl River T0 and mesocosms. Corresponding colors legend is valid for all brGDGT figures as well.

tracked. First, the variation in control mesocosms will be evaluated to test H1. As the mesocosms have narrow pH ranges (7–8.5) and conductivity (~200–300 μS/cm), temperature is the main parameter changing in the mesocosms, which will allow to test for H2. By determining the impact of several water chemistry parameters (Supp. Table 3) on brGDGT concentration and distribution, the mesocosms provide the opportunity to evaluate whether temperature changes have a stronger impact on brGDGTs than changes in water chemistry (H3).

3.2. DNA quantification and sequencing data

To identify the bacteria community composition in our incubations that could be responsible for brGDGTs distribution variability and address (H4), the composition of the bacterial community is determined (Supp. Table 1).

For the individual T0 conditions, the composition of the 20 most abundant phyla and Acidobacteria is summarized in Supp. Fig. 3. With a fractional abundance of 36% of total reads, phylum Proteobacteria is the most abundant bacteria in both sites, followed by phylum Actinobacteriota with 25% of all rarefied reads. In Lake Rot T0, Actinobacteria ($\overline{x}$=49%, σ = 21%) and Proteobacteria ($\overline{x}$=24%, σ = 11%) are the most common phyla in all seasons. In Sihl River, phylum Bacteroidota is the most abundant in spring (43%) while in summer and autumn, Proteobacteria has the highest total reads (43%, 42%) respectively. Phylum Acidobacteriota, whose members are shown to produce brGDGTs (Sinninghe Damsté et al., 2018; Chen et al., 2022; Halamka et al., 2022), is represented in all samples with a low fractional abundance (<2%, LR:1–35, SR: 20–44 reads), with an increased occurrence in autumn

(LR:35, SR:124 reads). OTUs that are typical for either Lake Rot or Sihl River (bio-indicator OTUs) have been determined (Supp. Fig. 4). As represented in Supp. Fig. 3, there is significant variability in bacterial community composition after the start of the mesocosms in both Lake Rot and Sihl River over time and between treatments (control/cooling/warming). To summarize significant changes in bacterial composition, bacterial OTUs that are increased significantly in mesocosms with high MBT'$_{5ME}$ in Lake Rot and increased IR in Sihl River are reported, after removing 5 OTUs that are potential contaminations. These OTUs are placed within the phyla Acidobacteria (Vicinamibacteria and Blastocatellia), Actinobacteriota (order Frankiales), Gammaproteobacteria (Burkholderiales), and Planctomycetota (order Planctomycetes and Phycisphaerae) for Lake Rot. For Sihl River 87 bio-indicator OTUs are identified within Actinobacteriota (order Microtrichales and Frankiales), Alphaproteobacteria (orders Acetobacterales, Caulobacterales, Reyranellales, and Rhodobacterales), Bacteroidota (order Chitinophagales), Cyanobacteria, Gammaproteobacteria (order Burkholderiales and Salinisphaerales) and Patescibacteria (Candidatus_Kaiserbacteri), Planktomycetota (order Pirellulales).

Changes in the bacterial community in control mesocosms will be described to test H1. With a distinct bacterial community between Lake Rot and Sihl River and described changes in the community composition with time, the bio-indicators identified will allow us to evaluate whether changes in bacterial community composition affect the brGDGTs ratios (H4).

3.3. BrGDGT concentration and distribution

3.3.1. Environmental distribution (T0)

Comparing brGDGT concentration at initial conditions (T0) (Fig. 3), brGDGTs were present at a high concentration in spring in Lake Rot and Sihl River (114 and 335 ng/L, respectively). In summer and autumn, both sites have noticeably lower brGDGT concentrations (generally < 60 ng/L, Fig. 3, one-way ANOVA with p < 0.001). In addition to concentration changes, T0 brGDGT distribution is distinct between seasons. In Lake Rot, MBT'$_{5ME}$ values increase from spring (0.41) to summer and autumn (0.48 and 0.44, respectively), reflecting a proportional increase of the fractional abundance of brGDGT Ia, compared to IIIa with increasing MBT'$_{5ME}$ values (Supp. Table 2). This contrasts with Sihl River, where the MBT'$_{5ME}$ values in summer (0.44) and autumn (0.42) are slightly decreased compared to spring (0.48). Similarly, the change in T0 MBT'$_{5ME}$ values can mainly be tracked through changes in the fractional abundance of Ia compared to IIIa.

Similar to MBT'$_{5ME}$, variation in IR values between seasons is observed. Lake Rot summer IR (0.52) is decreased, compared to spring and autumn values (both 0.63), caused by a relative increase in brGDGT IIIa compared with IIa' and IIIa' in summer. In Sihl River, IR values are 0.38 for all seasons, representing stable fractional abundances of brGDGTs IIa, IIIa, IIa' and IIIa' (Supp. Table 2). Seasonal variation in distribution of GDGTs in T0 will be used to test H2.

3.3.2. Mesocosm distribution changes

The variation in the concentration and distribution of brGDGTs in the control, cooling, and warming treatments is evaluated to determine the stability of control mesocosms and the impact of temperature on brGDGT ratios (H1 and H2). Water collected at each starting condition contained viable GDGT producers, as the concentration of summed brGDGTs, compared to T24h, showed an initial increase after the beginning of the experiment, generally followed by a decrease in concentration (Fig. 3). In several mesocosm bottles the brGDGT concentration is increased compared to T0 (or T24h), 29 (40%) and 31 (52%) of Lake Rot and Sihl River, respectively. For those bottles where the summed concentration remained stable or decreased, a change in brGDGT distribution was considered to reflect the production of at least 1 brGDGT compound. With this selection process, summarized in Supp. Table 4, only 9 mesocosm bottles (all from Lake Rot) showed no evidence of brGDGT production, and were removed from the dataset, keeping 156 (86%) of all mesocosm bottles for GDGT description and discussion. GDGT distribution and concentration of either non-duplicate or average values of duplicate mesocosms are reported in Supp. Table 2.

In Lake Rot mesocosm (Fig. 4A) control treatments, the

concentration of brGDGTs generally decreases with time (however no negative correlation is present). In the temperature treatments, individual 5-methyl brGDGT compounds show distinct concentration changes with time, often specific for individual seasons. Specifically, the concentration of brGDGT Ia and IIa (ng/L) increase the strongest in spring warming treatments (25 °C) with timepoints (r = 0.95, 0.96, p = 0.05, respectively, Fig. 4A, orange bars). The concentration of brGDGT Ia also increases with time in the warming incubations (excluding T3W) of the autumn season (r = 0.65, p < 0.2, Fig. 4A, brown bars). In cooling treatments of summer and autumn, brGDGTs IIa and IIIa exhibit comparable concentration change through time, reflecting an initial increase followed by a decrease at T2W. In control treatments, the concentration of brGDGTs generally decreases with time (however no negative correlation is present). Because individual brGDGTs show different concentration variations in Lake Rot mesocosms, the fractional abundances of major brGDGTs Ia, IIa and IIIa vary between temperature treatments (Fig. 5A). The increase in GDGT concentration and change in their distributions and GDGT-based ratio in both control and temperature treatment experiments will be discussed when testing H1 and H2. To address the temperature impact on GDGT ratios (H2), the MBT'$_{5ME}$ and IR values are calculated.

As MBT'$_{5ME}$ values are expected to respond to temperature, MBT'$_{5ME}$ changes in the different temperature treatments are reported (control, cooling, warming; Supp. Table 2). With a range of 15–60 %, brGDGT Ia has the highest fractional abundance across treatments of Lake Rot. In cooling incubations, the changes in fractional abundances of Ia and specially IIIa are limited in (Fig. 5A). A decrease in MBT'$_{5ME}$ values is observed only for the last timepoint of the autumn season (T5W, Fig. 6A), driven by a sudden increase in the fractional abundance of IIIa (Fig. 5A). However, at the final time point (T5W) a significant reduction in the concentration of brGDGTs is observed compared to the initial conditions, where brGDGTs Ia and IIa fall below detection limit. Although degradation of individual compounds is not expected to influence the distribution (Yamamoto et al., 2016), changes in the composition can be caused by degradation.

In contrast, in the autumn warming incubation, Ia % increases and IIIa decreases (going below the detection limit with time), reaching a final value of 0 at 5 weeks (T5W). Hence, the MBT'$_{5ME}$ values increase with time in the autumn season (r = 0.97, p < 0.05, excluding T3W). Also, in individual mesocosms of the spring warming treatments (Fig. 6A) MBT'$_{5ME}$ values are increased, caused by elevated Ia % and IIa %. In Lake Rot control incubations, the fractional abundance of Ia marginally increases with time in spring mesocosms as reflected in the MBT'$_{5ME}$ increase in these incubations. In summer and autumn, the variation in MBT'$_{5ME}$ values is muted in control treatments, with
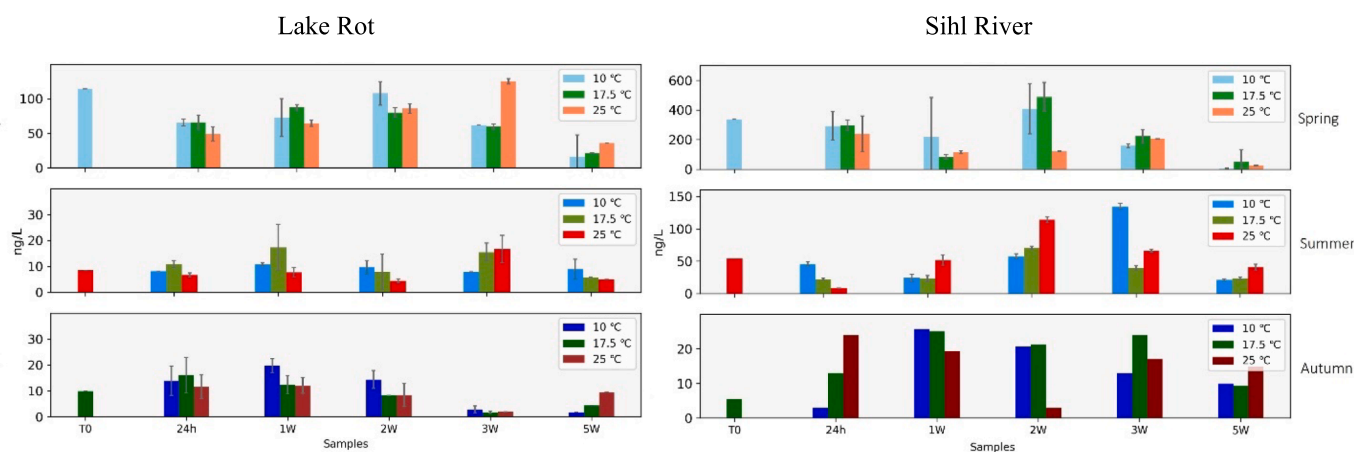

Fig. 3. Bar plots of summed concentration of brGDGTs from Lake Rot and Sihl River, with top, middle and bottom panels representing spring, summer and autumn, respectively. T0 values present concentration of brGDGTs filtered at site, timepoint values represent mesocosm samples filtered at each timepoint. Error bars reflect the standard deviation from mesocosm duplicates, with Sihl river autumn having no duplicate values.
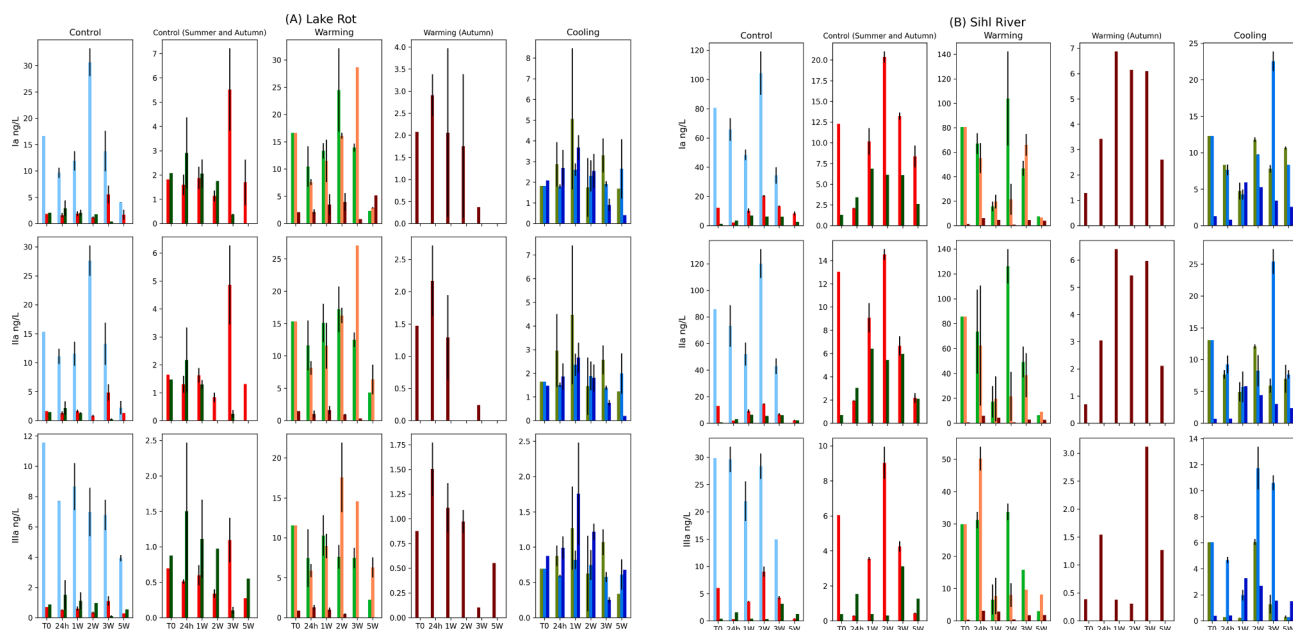
Fig. 4. Bar plots representing concentrations of individual brGDGTs Ia, IIa and IIIa in (A) Lake Rot and (B) Sihl River T0 and temperature treatment (control, cooling, and warming) mesocosms. Because of lower concentrations, subpanels "summer and autumn" and "autumn" present the values for these seasons on a magnified y-axis. Error bars reflect the standard deviation of mesocosm duplicates, with Sihl river autumn having no duplicate values. See Fig. 2 for the color legend for this Fig.

Fig. 5. Line plots of fractional abundance of brGDGTs Ia, IIa, IIIa, IIa' and IIIa' in (A) Lake Rot and (B) Sihl River T0 and mesocosms. Error bars reflect the standard deviation of mesocosm duplicates, with Sihl river autumn having no duplicate values.. See Fig. 2 for the color legend for this Fig.
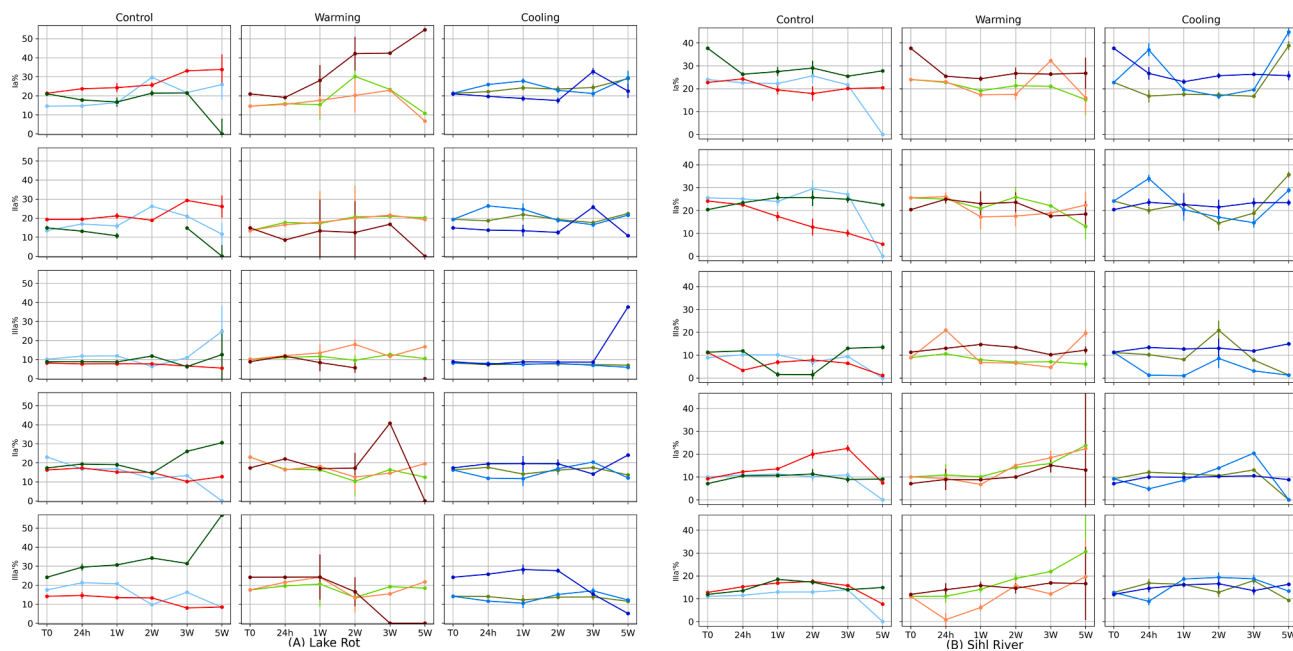
diverging MBT'$_{5ME}$ values observed at T5W (Fig. 6A).

In Lake Rot mesocosms, the concentration of 6-methyl brGDGTs (ng/L) represents stable values in all individual temperature treatments (control, cooling and warming) of spring and summer (Fig. 7A). In autumn cooling and warming incubations, however, compound IIIa' gradually decreases and is present below detection limit at end of the experiment. The increased fractional abundance of brGDGT IIa' in some mesocosms of Lake Rot (i.e., autumn warming T3W), is not caused by a concentration increase of this compound but instead a decrease of IIIa'. For T ≤ T2W of Autumn control mesocosms, the fractional abundance of 6-methyl compounds is higher (25–40%), which is not observed in

spring and summer control incubations (10–20%). This is reflected in the variability in autumn IR values (Fig. 6A), where in autumn control and warming incubations, IR remains high (IR > 0.6) for T ≤ T3W. In the cooling treatment of autumn however, with a decrease in fractional abundance of brGDGT IIIa', IR decreases after T2W. In general, changes in the fractional abundance of 6-methyl GDGTs and the IR values are mainly driven by both 5-methyl and 6-methyl compounds.

In Sihl River mesocosms, the response of brGDGTs to temperature treatments is distinct from Lake Rot. The concentrations of brGDGT Ia, IIa and IIIa do not exhibit a uniform increase or decrease in any of the warming or cooling treatments (Fig. 4B), although there is variability in
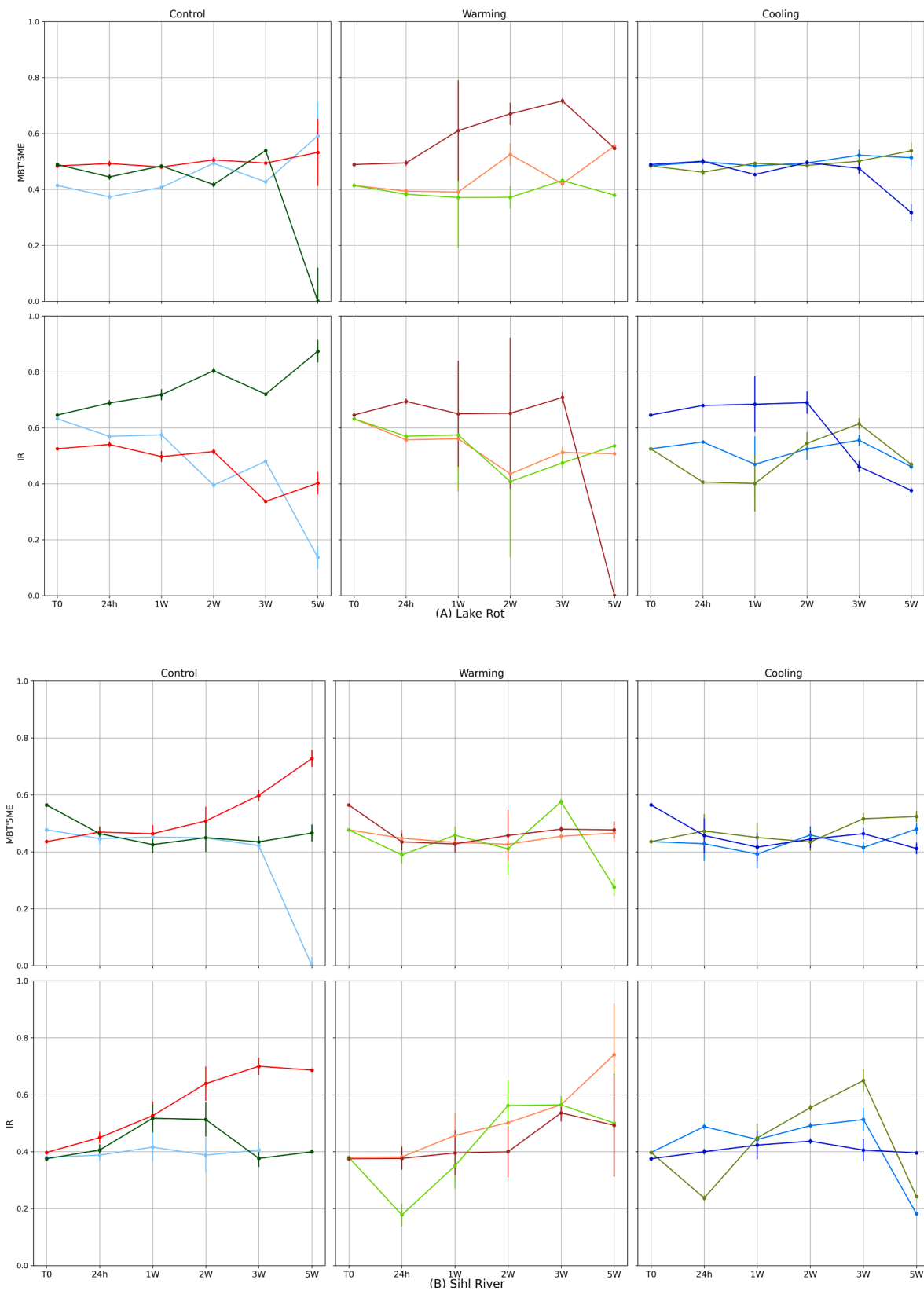
Fig. 6. Line plots displaying the brGDGT ratios MBT'$_{5ME}$ and IR for (A) Lake Rot and (B) Sihl River T0 and mesocosms. Error bars reflect the standard deviation for mesocosm duplicates. See Fig. 2 for the color legend for this Fig.
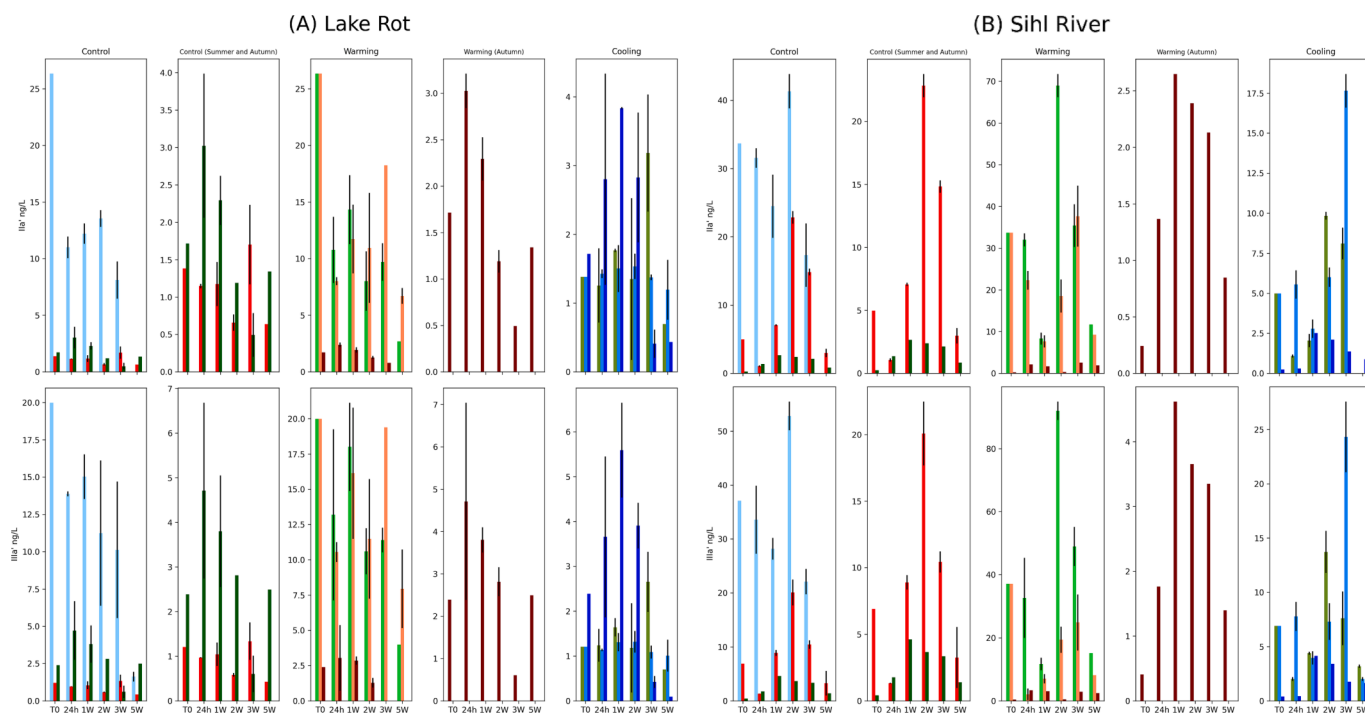
Fig. 7. Bar plots showing the concentration of individual 6-methyl brGDGTs IIa' and IIIa' in (A) Lake Rot and (B) Sihl River T0 and temperature treatment (control, cooling, and warming) mesocosms. magnified subpanels "summer and autumn" and "autumn" present the values for these seasons on smaller y-axis. Error bars reflect the standard deviation of mesocosm duplicates. For Autumn Sihl River, presented values are based on single measurements (no error bars). See Fig. 2 for the color legend for this Fig.

GDGT concentration and a good agreement in concentration changes between brGDGT Ia vs IIa ($R^2 = 0.50$, 0.72, for warming and cooling, respectively). In spring and autumn control treatments, the variation in the fractional abundances of brGDGTs Ia, IIa, IIIa (Fig. 5B) results in minimal changes in MBT'$_{5ME}$ values (Fig. 6B). However, MBT'$_{5ME}$ increases in the summer control treatments, driven by a decrease in the fractional abundance of brGDGT IIa (although not observed in concentration of IIa compared to Ia). In the cooling treatments, no response of the MBT'$_{5ME}$ with time is observed, although the variance in the summer cooling treatment (17.5 °C) increases with time (Fig. 6B). In the warming treatment (25 °C), spring MBT'$_{5ME}$ values increase in individual mesocosm bottles, driven by an increase in brGDGT Ia fractional abundance (although minimally observed in the concentration of IIa compared to Ia). In addition to the 5-methyl brGDGTs, the concentrations of 6-methyl compounds are variable in both the control and temperature treatments. Except for the concentration of IIIa', which increases with time in the warming (25 °C) treatments of spring ($r = 0.98$, $p < 0.05$), generally 6-methyl brGDGT concentrations do not display a uniform trend with time. Reflecting the increase in concentration, brGDGT IIIa' fractional abundance increases with time in spring warming (17.5 °C and 25 °C) treatments ($r = 0.97$, $r = 0.98$, $p < 0.05$, respectively, Fig. 5B). The fractional abundance of 6-methyl brGDGT IIa' increases with time (excluding T5W) in control and cooling (17.5 °C) treatments in summer ($r = 0.97$, 0.99, $p < 0.05$, respectively for control and cooling; Fig. 5B), and in autumn ($r = 0.82$, $p < 0.1$) and spring (17.5 °C) warming treatments ($r = 0.96$, $p < 0.05$), resulting in IR values that increase with time in spring warming treatment (17.5 °C) ($r = 0.96$, $p < 0.05$, Fig. 6B).

Across both sites and all seasons, MBT'$_{5ME}$ thus increases with time in 2 warming treatments, specifically Lake Rot spring (17.5 °C) and Lake Rot autumn (25 °C), and in the control treatments of Lake Rot spring and Sihl River summer. It does not increase or decrease in any cooling treatments. While the MBT'$_{5ME}$ is the most temperature-sensitive proxy in Lake Rot, in Sihl River, IR represents the prominent temperature dependencies. As such, the discussion will explore the mechanisms

behind the temperature-dependent variation in MBT'$_{5ME}$ and IR values of Lake Rot and Sihl River.

4. Discussion

4.1. Performance of mesocosms for brGDGTs production

To evaluate whether control incubations were representative of natural conditions (H1), changes in chemistry, bacterial community and GDGTs are discussed. In both the control incubations of spring and autumn in Lake Rot and Sihl River, the chemistry variables (including pH, alkalinity, conductivity, and Ca^{2+}) partially exhibit limited variability with time, but only across a small range (pH up to 0.25, alkalinity up to 35, conductivity up to 25, Ca^{2+} up to 250; Supp. Fig. 5). The control treatment therefore did not impact inorganic chemistry values strongly compared to initial natural conditions (T0). The NMDS plot of the control samples (Supp. Fig. 6) reveals limited but existing variability in the composition of the bacterial community, especially in the single successfully characterized sample taken at T5W. This suggests that while some changes are evident in the control incubations, the majority of the bacterial community exhibits a relatively consistent composition, indicating a limited degree of succession under control conditions.

Variations in GDGTs concentration (2–5 fold increase/decrease) and ratio (0.1–0.2 unit change in MBT'$_{5ME}$) were observed in the control treatments for all seasons at both sites (Supp. Fig. 7). This change in concentration aligns with the variability reported by Martínez-Sosa and Tierney (2019) in concentration (2–4 fold change) and ratios (0.1–0.4) of their samples and can be attributed to possible increased biovolume in bacteria when relieved from grazing pressure in the mesocosm bottles (Pomeroy et al., 1994; García-Martín et al., 2011; Kunzmann et al., 2019). Observing this response in the control mesocosms shows that it is a temperature-independent effect. It is advisable to exercise caution when interpreting the initial changes in bacterial community composition and brGDGT concentration and distribution considering the so called "bottle effect". This term refers to errors arising from sample

containment. As such samples will practically capture only part of the natural community, excluding for instance grazers, this leads to changes in community composition and interactions (Pomeroy et al., 1994). Based on the control mesocosms, initial changes in the mesocosms can thus be attributed to the release of the grazing pressure. In addition, the controls indicate that after 5 weeks the bacterial communities undergo drastic changes that can be related to nutrient limitations. Furthermore, based on results from Martínez-Sosa and Tierney (2019), it takes 2–4 weeks before the background GDGT signal is overwritten and no instantaneous responses to the temperature change are thus expected. Consequently, although changes across all timepoints are discussed, the mesocosms that have had more time for acclimation (e.g., T2W, T3W) to the experimental temperature tests, may represent the most realistic response to temperature change.

4.2. In-situ seasonal brGDGT signatures

The brGDGT concentrations in Lake Rot summer and autumn T0 measurements ($10 > \Sigma brGDGT > 8$ ng L^{-1}) compare well with other freshwater lakes, namely, Lower King Pond and Lake Chala ($\Sigma brGDGT < 12$ ng L^{-1}, Loomis et al., 2014, Van Bree et al., 2020, respectively). Similarly, summer T0 brGDGT concentration in Sihl River ($\Sigma brGDGT = 54$ ng L^{-1}) is comparable with reports of brGDGT concentration from Yenisei River in east Siberia ($\Sigma brGDGT < 69$ ng L^{-1}, collected in summer, De Jonge et al., 2014a). However, in eutrophic Lake Rot and Sihl River, brGDGTs spring in situ concentrations (LR-$\Sigma brGDGT = 114$ ng L^{-1}, SR-$\Sigma brGDGT = 335$ ng L^{-1}) exceed those reported in other lake and riverine systems (Martínez-Sosa et al., 2020; Van Bree et al., 2020). With comparable in situ MBT'$_{5ME}$ values (0.41–0.48) across all seasons for both sites, the absolute values (12–14 °C) are comparable to the real-time day average air temperatures (8.4–10.3 °C). However, the small variability in reconstructed temperature (T$_{rec.}$) between seasons does not reflect the seasonal variability of in situ temperatures in both calibrations applied. Reconstructed temperatures derived from both Russell et al. (2018) and the average reconstruction from Martínez-Sosa et al. (2021) (Supp. Table 2) showed an offset of less than 2 degrees. The reported values are based on the Russell et al. (2018) calibration, as the in-situ measured temperatures generally were closer to this calibration. Spring and autumn reconstructed temperatures (Lake Rot: 12 °C and 14 °C, Sihl River: 14 °C and 12 °C) present an offset of 2 to 3 °C in spring and of 2 to 5 °C in autumn (measured air temperature of 8.4 °C and 10.3 °C in spring and 18.2°C and 14.4 °C in autumn for Lake Rot and Sihl River, respectively). This offset is bigger (6 to 10 °C) for summer, where measured in situ air temperature is 20.5 °C for Lake Rot (reconstructed temperature = 14 °C), and 22.1 °C for Sihl River (reconstructed temperature = 13 °C), respectively. This muted variation in T0 MBT'$_{5ME}$ values across seasons indicates that brGDGT producers in these systems are less sensitive to temperature changes, compared to what would be expected based on a global scale.

4.3. Impact of temperature on brGDGT distribution

Based on global calibrations we expect the MBT'$_{5ME}$ to increase with warming, decrease with cooling and remain stable in control conditions, with step-sizes reflecting the variability present on the global scale (H2). In Lake Rot mesocosms, the variations in MBT'$_{5ME}$ followed this response only in a subset of the treatments (Fig. 6A). In the autumn warming treatment, an increase in Ia concentration and a decrease in IIIa causes the MBT'$_{5ME}$ to increase with temperature, reaching 0.71 (T$_{rec.}$ = 22 °C) at T3W before dropping to 0.55 (T$_{rec.}$ = 16 °C) at T5W. The temperature dependency of brGDGTs in the autumn season is confirmed by the observation that the fractional abundance of brGDGT IIIa increases in the cold treatment, resulting in a decrease of the MBT'$_{5ME}$ (0.32), with a reconstructed temperature (9 °C) similar to the cold incubation temperature (10 °C). A second example of MBT'$_{5ME}$ increases in response to warming is observed in one of the warming

incubations (17.5 °C) of spring, where MBT'$_{5ME}$ values reach 0.56, reflecting reconstructed temperatures (16.8 °C) that are similar to the growth temperature. The increase of MBT'$_{5ME}$ values aligns with a similar trend observed in mesocosms in a warm lake (AZ, USA) where, after 4–6 weeks of incubation at warmer temperatures (27 and 35 °C), MBT'$_{5ME}$ values consistently increased with up to 0.5 MBT'$_{5ME}$ units (Martínez-Sosa et al., 2020). However, in the Swiss mesocosms the response size is generally smaller (up to 0.3). Furthermore, the lack of response in some of our warming mesocosms is not observed at the warm Lake Kennedy mesocosms (Martínez-Sosa et al., 2020). Indeed, not all temperature and control treatments result in the expected response of the MBT'$_{5ME}$. In the warmest spring warming (25 °C) treatment, where the concentration of Ia shows a steady increase with time, MBT'$_{5ME}$ does not increase. Ia concentration is indeed matched by an increase in the concentration of IIa and IIIa, which results in stable MBT'$_{5ME}$ ratio values instead. In addition to an increase in the warming treatment, in the spring control treatment, the MBT'$_{5ME}$ shows a muted but significant increase with time (r = 0.83, p < 0.1), caused by a higher fractional abundance of Ia, IIa, Ib and Ic (Supp. Table 2; Fig. 5A for Ia and IIa). There is thus seasonal variation in the temperature dependence of brGDGTs, with significant changes in the MBT'$_{5ME}$ in autumn caused by changes in concentration and the fractional abundances of 5-methyl brGDGTs Ia and IIIa, while more muted changes in the spring season are caused by the increased concentrations and fractional abundances of brGDGTs Ia and IIa.

Although MBT'$_{5ME}$ is seen to increase in several warming but also control treatments, a decrease of MBT'$_{5ME}$ values in cooling treatments is never observed (apart from Autumn T5W), exemplified by the summer incubations where MBT'$_{5ME}$ shows a low variability ($\bar{x}$=0.5, σ = 0.02). This could indicate a limited response of brGDGTs producers to cooling temperatures, as bacterial activity is temperature-dependent (White et al., 1991). Still, even a slow decrease in MBT'$_{5ME}$ values is not detected. This observation is consistent with the findings in the cooling mesocosms of Lake Kennedy, where MBT'$_{5ME}$ also does not exhibit a decrease over time in incubations conducted at lower temperatures (9 and 18 °C), compared to their the in-situ environment (22 °C).

This absence of consistent increase/decrease in the fractional abundance of brGDGTs Ia and IIa or IIIa and the MBT'$_{5ME}$ values in all warming incubations (Fig. 5A, Fig. 6B) challenges the proposed temperature dependency of these compounds in Lake Rot. In addition to the temperature dependency of the MBT'$_{5ME}$, we evaluate the temperature sensitivity of the IR. Tentative positive correlations between the IR and temperature based on large regional to global scale datasets have been put forward recently by Russell et al. (2018) and Martínez-Sosa et al. (2021) but were not reported as such by Raberg et al. (2021). In Lake Rot, the concentration of 6-methyl compounds (IIa', IIIa') increases with time in temperature treatments, specifically some of the autumn cooling incubations, supporting the idea of a potential aquatic producer of 6-methyl brGDGT during autumn. In some warming treatments (autumn), an increase in the fractional abundance of IIa' is observed, but it is not caused by a clear increase in the concentration of brGDGT IIa'. An increase in IR values with time in the warm treatments is not observed (Fig. 6A).

Compared to lakes, the dependency between MBT'$_{5ME}$ values and temperature in rivers is poorly constrained. Although the occurrence of in situ produced brGDGTs has been reported in river systems (De Jonge et al., 2014a; Zell et al., 2014; Kirkels et al., 2022), it remains unclear whether 5-methyl brGDGTs produced in fluvial systems show the same temperature response as brGDGTs produced in lakes. Instead, 6-methyl brGDGTs have been proposed to be indicative of in-situ production in rivers (Freymond et al., 2017; Kirkels et al., 2022). To test the temperature response of riverine brGDGTs, freshwater from Sihl River was subjected to the same temperature treatments as Lake Rot.

Only in the summer treatments, the MBT'$_{5ME}$ values in the control incubations, which are only 2–3 °C warmer than in situ summer temperatures, portray a positive correlation (r = 0.54) with time, reaching a

final (T5W) reconstructed temperature of 22.1 °C, representing real-time summer in situ temperature. This elevated MBT'$_{5ME}$ trend is reflected in the increase in fractional abundance of brGDGT Ia at a higher rate compared to IIa and IIIa (Fig. 5B). However, other than the concentration increase of brGDGT Ia in the summer control treatment, and a sporadic increase in the concentration of brGDGT IIIa in some incubations of spring warming treatment (25 °C), in general, 5-methyl brGDGTs show no concentration changes in Sihl River temperature treatments (Fig. 6B).

Instead, the majority of brGDGTs variation is observed as changes in the 6-methyl brGDGTs, and correspondingly the IR values (Fig. 6B). With the observed strong concentration increases of 6-methyl compounds in Sihl River mesocosms (especially in spring and summer), aquatic production of these compounds is confirmed, leading to changes in the fractional abundance of brGDGTs. In spring, the fractional abundance of 6-methyl brGDGTs increase in warming treatments while remaining stable in the control treatment, indicating that temperature potentially has a direct effect on the production of IIa' and IIIa'. Supporting the production of 6-methyl brGDGTs at warm temperatures is the observation that in summer incubations IIa' and IIb' also increase in concentration with time (T24h to T2W) in control treatments, i.e., at a warm growth temperature. On the other hand, the concentration of brGDGT IIIa', shows a 3-fold increase with time (T24h-T3W) in the coldest treatment (10 °C) of summer, potentially reflecting an increase in hexamethylated brGDGTs when growth temperature drops strongly (here: 15 °C), and complicating the interpretation of temperature-dependence of this compound. In autumn, IR stays stable across different treatments with only the warming treatment (T > 2 W) showing a marginal increase in IR. As the temperature dependency of the fractional abundance of the 6-methyl brGDGTs and the IR is not uniform across temperature treatments and seasons, its application as a temperature proxy will be limited. However, its use as a proxy for in situ production of brGDGTs in river systems, a process that is expected to be more intense when the temperature is warmer, is confirmed.

Across both sites, the response of either MBT'$_{5ME}$ or IR on the temperature treatments reveals a temperature dependency that is dominated by a response to warming, and absent or muted responses to cooling. This different temperature dependency of brGDGTs in fluvial and lacustrine settings can possibly impact the interpretation of the MBT'$_{5ME}$ as a temperature proxy in sedimentary settings with substantial riverine input. The increase in concentration or fractional abundance of IIa' in warmer conditions (Figs. 5, 6), however, is shared between both sites presenting similarities in response of 6-methyl compounds to temperature irrespective of their aquatic source. Still, although the MBT'$_{5ME}$ (in Lake Rot) and IR (in Sihl River) reflect a temperature dependency, not all variation in these proxies can currently be explained by the temperature treatments.

4.4. Impact of water chemistry on brGDGT variability

Although the mesocosm experiment aimed at keeping all other environmental variables constant to measure the impact of temperature, some variability in the inorganic water parameters is observed (Fig. 2). This variability can be explained by evaporation (conductivity and cation concentrations increase with time in some mesocosms), and a possible difference in the suspended mineral content (impacting cation concentrations) between mesocosm bottles during filling the mesocosm bottles. Furthermore, temperature can also accelerate chemical reactions in freshwater (Elser et al., 2007), potentially changing the mineral content concentrations of individual mesocosms. As for instance conductivity (Tierney et al., 2010; Shanahan et al., 2013; Loomis et al., 2014; Raberg et al., 2021) and nutrient availability (Loomis et al., 2014) have been reported to potentially control the brGDGTs distribution, these unintended changes in water chemistry have potentially impacted the brGDGT ratios. To statistically test for the impact of confounding parameters in addition to temperature, a factorial design should have

been used (e.g., Collins et al., 2009). As this was not the case, we address H3 by performing a post hoc analysis of the variability of GDGTs and water chemistry, for Lake Rot and Sihl River separately.

As T0 water chemistry of spring and summer had comparable values at both sites, we look at common dependencies that act across these two seasons collectively, while keeping autumn as a separate season, generating 12 correlation matrices (2 locations, 2 season groups, and 3 treatments (control, cooling and warming); Supp. Table 3A-B). In Lake Rot treatments, minimal correlations between brGDGT ratios and the inorganic parameters are observed, as is evident in the lack of a significant correlation between MBT'$_{5ME}$ and water chemistry. Concerning the proxies that vary with chemistry in soils (CBT' and DC'; Naafs et al., 2017; De Jonge et al., 2021), only DC' increases in multiple treatments with pH (Supp. Table 3A). Although DC' does not correlate with dissolved Ca^{2+} in warming incubations of Lake Rot (spring and autumn), the fractional abundance of IIb' correlates with dissolved Ca^{2+} (r = 0.74), which matches the previously described increase of 6-methyl brGDGTs with exchangeable Ca^{2+} in soils (Halffman et al., 2022). However, as DC' does not respond to pH in all mesocosm studies, and the dependency of IIb' on Ca^{2+} is not observed in control and cooling mesocosms, although a range in pH and Ca^{2+} values is present, the environmental dependency of the DC' remains poorly constrained based on the Lake Rot mesocosms.

In Sihl River, however, multiple brGDGT ratios and fractional abundances of brGDGTs correlate with temperature and water chemistry (Supp. Table 3b), and we first discuss whether water chemistry drives variation in the IR, in addition to the temperature dependency. IR values correlate with water pH in summer cooling incubations (r = 0.72), which matches previous observations in soils (Naafs et al., 2017; Russell et al., 2018; De Jonge et al., 2021). The correlations between the fractional abundance of IIIa' and IIa with pH (r = 0.65, r = –0.66, respectively) cause the dependency between IR and pH. A more general dependency is observed between IR and water conductivity in control (spring and summer) and cooling (summer) incubations (r = 0.70, r = 0.72, respectively), which is based on correlations between conductivity and the fractional abundance of IIa (r = -0.73, r = –0.74, respectively), and 6-methyl compounds IIa' (Supp. Table 3B). This observation supports the correlation between IR and conductivity previously reported by Raberg et al. (2021). However, it is not observed in all mesocosms.

Similar to Lake Rot, in the cooling treatments of Sihl River (n = 10), DC' increases with water pH (r = 0.73), as does the fractional abundance of brGDGT IIb' (Supp. Table 3B), but not Ib or IIb compounds, promoting the idea of a strong impact of water pH on the 6-methyl cyclopentane containing brGDGT IIb' in freshwaters of both lakes and rivers. This observation is in general agreement with previously reported positive correlations of fractional abundances of monocyclopentane containing brGDGTs (Ib, IIb, IIb') and pH in lake sediments (Raberg et al., 2021).

In our seasonal dataset, multiple distinct correlations between brGDGTs ratios and inorganic environmental parameters are observed, particularly in Sihl River. However, no overarching driver of aquatic chemistry on brGDGT ratios could be identified. Based on the mesocosm studies, where the range in water chemistry values is minor and well-constrained, variations in the brGDGTs distribution are predominantly attributed to temperature changes. Nonetheless, our findings suggest that chemical environmental factors, particularly in riverine systems, can have the potential to affect brGDGTs ratios typically used for chemistry or conductivity reconstruction (IR, DC').

4.5. Bacterial community composition as a source of brGDGT variability

As several brGDGTs and brGDGT-based ratios showed variability in response to environmental drivers, coeval compositional changes in the bacterial community can be evaluated to constrain potential GDGT producers. As this is based on relative quantities, e.g., rarefied 16S rRNA gene counts, including strains that don't produce brGDGTs, we report

correlations between brGDGT ratios and bacterial groups that show relative increases, without assigning bacterial groups as definite brGDGT producers.

In soils, large changes in the MBT'$_{5ME}$ ratio and the IR have been attributed to changes in the composition of the bacterial community (De Jonge et al., 2019; De Jonge et al., 2021). To elucidate whether a similar mechanism can explain the variation in brGDGT distribution, we use a bio-indicator approach. As the bacterial community composition for each T0 is different, we report significant changes in the fractional abundance of OTUs per season that are coeval with changes across a cut-off value in MBT'$_{5ME}$ values (for Lake Rot) and IR values (for Sihl River) for those seasons where 16S-based community composition was reconstructed in sufficient samples. The cut-off values are determined to represent an average value of the selected treatment.

Specifically, we determine bio-indicators in Lake Rot autumn mesocosms (n = 5, cut-off value of MBT'$_{5ME}$ = 0.50) and in the Sihl River spring mesocosms (n = 6, cut-off value of IR = 0.39). Firstly, in Lake Rot autumn, where a response of the MBT'$_{5ME}$ values with warming is observed (MBT'$_{5ME}$ ranges between 0.48 and 0.67), driven by a concentration increase of brGDGT Ia and a decrease of IIIa, we evaluate which bio-indicator OTUs are present in mesocosms with an elevated MBT'$_{5ME}$ value (>0.5, n = 2), compared to background values (0.48–0.50, n = 3). The phylogenetic distribution of the OTUs that are increased in high MBT'$_{5ME}$ mesocosms is represented by Actinobacteriota (order Frankiales and Micrococcales), and

A. MBT'$_{5ME}$ bio-indicators in LR Autumn, MBT'$_{5ME}$ >0.50

nOTU = 13

B. IR bio-indicators in SR Spring, IR >0.39
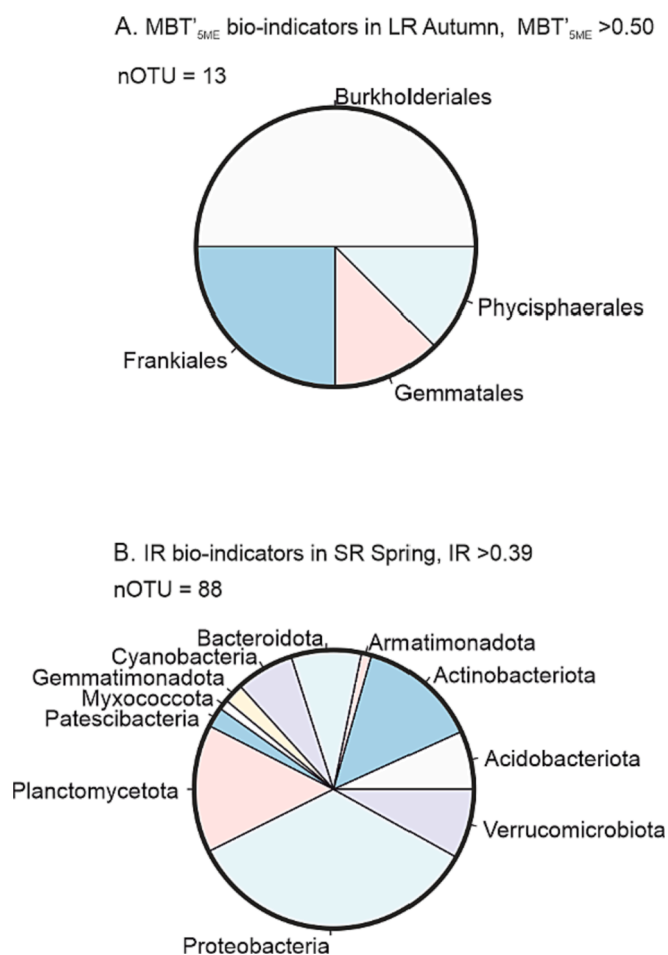
nOTU = 88

Fig. 8. Pie chart depicting the phylogenetic distribution of bio-indicator OTUs, (A) bio-indicator OTUs that are increased in Lake Rot autumn season mesocosms with MBT'$_{5ME}$ > 0.5, order level; (B) distribution of bio-indicator OTUs that are increased in Sihl River spring season mesocosms with IR > 0.39, phylum level.

Gammaproteobacteria (order Burkholderiales) [Fig. 8A]. Interestingly, no Acidobacterial OTUs were included in the bio-indicators. This aligns with previous observations of low abundance of Acidobacteria in freshwater settings, suggesting that sources other than Acidobacteria may potentially be responsible for brGDGT production in lakes. Evaluating the bio-indicators identified, Zeng et al. (2022) describe the presence of a Tes homologue in the genus Oxalobacteraceae (Burkholderiales). As such, this OTU (8 % of all reads) potentially contributes to the production of GDGTs in Lake Rot mesocosms. Secondly, IR bio-indicator OTUs are determined in the Sihl River spring mesocosms (n = 6, cut-off value of IR = 0.39), where brGDGT IIIa' shows variation in concentration. Several bio-indicator OTUs with a wide phylogenetic spread are determined (Fig. 8B). Among these, acidobacteriotal orders Vicinamibacteria (subgroup 6; 3 bio-indicator OTUs) and Blastocatellia (subgroup 4; 2 bio-indicator OTUs) have been shown to produce brGDGT precursor lipids (reviewed in Sinninghe Damsté et al., 2018) and to increase in soils with increased pH and IR values (De Jonge et al., 2021). Furthermore, representatives of the following orders have been shown to carry a Tes homologue (Zeng et al., 2022); Chitinophagaceae (4 bio-indicator OTUs), Saprospiraceae (1 bio-indicator OTU), Sphingobacteriaceae (2 bio-indicator OTUs) and Pirellulaceae (3 bio-indicator OTUs). These OTUs are generally present in low abundance, with the Sphingobacteriaceae bio-indicator OTUs as the most abundant clade, amounting up to 1.3 % of OTU reads.

Although changes in the fractional abundance of Acidobacterial OTUs can be responsible for the observed changes in IR in Sihl River, a) the low abundance of Acidobacterial bio-indicator OTUs (0 to 0.5%), b) lack of detection of Acidobacteria orders in Lake Rot bio-indicator OTUs, and c) the detection of several other bio-indicator OTUs in both Lake Rot and Sihl River imply that not all brGDGT producers may fall within this phylum. Further research aimed at identifying bacterial producers of brGDGTs in freshwater systems, should not only focus on identifying potential producers within the Acidobacteria phylum, but also explore other phyla that may be involved in the production of these biomarker lipids in freshwater systems.

5. Conclusions

The seasonal mesocosm dataset was used to test production of brGDGTs sourced from Lake Rot and Sihl River surface water under three different temperatures, providing insights into the drivers behind brGDGT variability in both lake and river systems. The hypotheses proposed can now be answered as follows:

(H1) While our oxic mesocosm setup revealed variations in brGDGTs concentration and/or distribution, evaluating the control set-ups highlighted that factors such as the removal of grazing microorganisms, change in nutrient availability, and the exclusion of sediment from freshwater introduce secondary effects, which limit the intent to which mesocosms can be seen as a replication of the natural environment. Furthermore, unintended small changes in the potentially confounding factors (pH, alkalinity, conductivity, Ca^{2+}) were measured, both in the control and in the temperature treatments, with specifically pH, alkalinity and conductivity showing correlations with GDGT-based ratios. To constrain the impacts of these parameters, a multifactorial design is needed. It is crucial for future incubation studies to exercise caution when considering the constraints of such setups and the potential sensitivity of specific microbial communities to temperature changes. Although the range of temperatures used was realistic, the sudden increase in temperature potentially impacted the MBT'$_{5ME}$ response for instance in the warmest spring mesocosm, and in the cold summer mesocosms. A modified set-up could include a more gradual increase or decrease of the growth temperature to test for this effect. Finally, employing more robust incubation setups like chemostats would enable continuous monitoring of nutrient availability for microorganisms, reducing nutrient stress for bacteria.

(H2) A muted increase in situ MBT'$_{5ME}$ values with temperature was

observed, with $T_{rec.}$ at both locations underestimating average temperature at time of sampling. The muted response of MBT'$_{5ME}$ in Lake Rot and Sihl River cooling and warming temperature treatments further highlights the limitations of this temperature proxy in our settings. Nonetheless, in certain mesocosms, MBT'$_{5ME}$ does show a response to warming temperatures.

(H3) Although water chemistry variables have the potential to affect brGDGT ratios (IR) in riverine systems, complicating the idea of a unidirectional temperature response of brGDGTs in the water column, temperature is still recognised as the primary driver behind brGDGT distribution changes. Therefore, the use of GDGT ratios as a paleotemperature application remains a reasonable and valuable approach.

(H4) A change in brGDGT distribution (specifically the IR in Sihl River) is indeed coeval with a change in bacterial community composition as revealed by the bio-indicator OTUs. This highlights the potential for the role of bacterial communities in driving changes in GDGT distributions.

In summary, the MBT'$_{5ME}$ is more strongly influenced by warming and may be insensitive to cold spells. Despite the observed limitation of MBT'$_{5ME}$ as a temperature proxy in Lake Rot and Sihl River, the increase in IR with warming temperature treatments in Sihl River suggests that the in-situ production of 6-methyl brGDGTs in rivers and their temperature sensitivity could be a promising area for further investigation.

Declaration of competing interest

The authors declare that they have no known competing financial interests or personal relationships that could have appeared to influence the work reported in this paper.

Data availability

Data will be made available on request.

Acknowledgement

Appendix A. Supplementary material

Supplementary data to this article can be found online at https://doi.org/10.1016/j.orggeochem.2024.104742.

References

Bódis, E., Tóth, B., Sousa, R., 2016. Freshwater mollusc assemblages and habitat associations in the Danube River drainage, Hungary. Aquatic Conservation: Marine and Freshwater Ecosystems 26, 319–332.

Buckles, L.K., Weijers, J.W., Verschuren, D., Sinninghe Damsté, J.S., 2014. Sources of core and intact branched tetraether membrane lipids in the lacustrine environment: Anatomy of Lake Challa and its catchment, equatorial East Africa. Geochimica et Cosmochimica Acta 140, 106–126.

Chen, Y., Zheng, F., Yang, H., Yang, W., Wu, R., Liu, X., Liang, H., Chen, H., Pei, H., Zhang, C., Pancost, R.D., Zeng, Z., 2022. The production of diverse brGDGTs by an Acidobacterium providing a physiological basis for paleoclimate proxies. Geochimica et Cosmochimica Acta 337, 155–165.

Collins, L.M., Dziak, J.J., Li, R., 2009. Design of experiments with multiple independent variables: a resource management perspective on complete and reduced factorial designs. Psychological Methods 14, 202.

De Cáceres, M. (2013). How to use the indicspecies package (ver. 1.7. 1). R Proj, 29.

De Jonge, C., Hopmans, E.C., Stadnitskaia, A., Rijpstra, W.I.C., Hofland, R., Tegelaar, E., Sinninghe Damsté, J.S., 2013. Identification of novel penta-and hexamethylated branched glycerol dialkyl glycerol tetraethers in peat using HPLC–MS2, GC–MS and GC–SMB-MS. Organic Geochemistry 54, 78–82.

De Jonge, C., Stadnitskaia, A., Hopmans, E.C., Cherkashov, G., Fedotov, A., Sinninghe Damsté, J.S.S., 2014a. In situ produced branched glycerol dialkyl glycerol tetraethers in suspended particulate matter from the Yenisei River, Eastern Siberia. Geochimica et Cosmochimica Acta 125, 476–491.

De Jonge, C., Hopmans, E.C., Zell, C.I., Kim, J.H., Schouten, S., Sinninghe Damsté, J.S., 2014b. Occurrence and abundance of 6-methyl branched glycerol dialkyl glycerol tetraethers in soils: Implications for palaeoclimate reconstruction. Geochimica et Cosmochimica Acta 141, 97–112.

De Jonge, C., Radujković, D., Sigurdsson, B.D., Weedon, J.T., Janssens, I., Peterse, F., 2019. Lipid biomarker temperature proxy responds to abrupt shift in the bacterial community composition in geothermally heated soils. Organic Geochemistry 137, 103897.

De Jonge, C., Kuramae, E.E., Radujković, D., Weedon, J.T., Janssens, I.A., Peterse, F., 2021. The influence of soil chemistry on branched tetraether lipids in mid-and high latitude soils: Implications for brGDGT-based paleothermometry. Geochimica et Cosmochimica Acta 310, 95–112.

Dedysh, S.N., Sinninghe Damsté, J.S., 2018. Acidobacteria. eLS, 1–10.

Deng, L., Bölsterli, D., Kristensen, E., Meile, C., Su, C.C., Bernasconi, S.M., Seidenkrantz, M., Glombita, C., Lagostina, L., Han, X., Jørgensen, B.B., Røy, H., Lever, M.A., 2020. Macrofaunal control of microbial community structure in continental margin sediments. Proceedings of the National Academy of Sciences 117, 15911–15922.

Elser, J.J., Bracken, M.E., Cleland, E.E., Gruner, D.S., Harpole, W.S., Hillebrand, H., Ngai, J.T., Seabloom, E.W., Shurin, J.B., Smith, J.E., 2007. Global analysis of nitrogen and phosphorus limitation of primary producers in freshwater, marine and terrestrial ecosystems. Ecology Letters 10, 1135–1142.

Freymond, C.V., Peterse, F., Fischer, L.V., Filip, F., Giosan, L., Eglinton, T.I., 2017. Branched GDGT signals in fluvial sediments of the Danube River basin: Method comparison and longitudinal evolution. Organic Geochemistry 103, 88–96.

García-Martín, E.E., Serret, P., Pérez-Lorenzo, M., 2011. Testing potential bias in marine plankton respiration rates by dark bottle incubations in the NW Iberian shelf: incubation time and bottle volume. Continental Shelf Research 31, 496–506.

Guo, J., Ma, T., Liu, N., Zhang, X., Hu, H., Ma, W., Peterse, F., 2022. Soil pH and aridity influence distributions of branched tetraether lipids in grassland soils along an aridity transect. Organic Geochemistry 164, 104347.

Halamka, T.A., Raberg, J.H., McFarlin, J.M., Younkin, A.D., Mulligan, C., Liu, X.L., Kopf, S.H., 2022. Production of diverse brGDGTs by Acidobacterium Solibacter usitatus in response to temperature, pH, and O2 provides a culturing perspective on br GDGT proxies and biosynthesis. Geobiology 21, 102–118.

Halffman, R., Lembrechts, J., Radujković, D., De Gruyter, J., Nijs, I., De Jonge, C., 2022. Soil chemistry, temperature, and bacterial community composition drive brGDGT distributions along a subarctic elevation gradient. Organic Geochemistry 163, 104346.

Han, X., Schubert, C.J., Fiskal, A., Dubois, N., Lever, M.A., 2020. Eutrophication as a driver of microbial community structure in lake sediments. Environmental Microbiology 22, 3446–3462.

Harning, D. J., Curtin, L., Geirsdóttir, Á., D'Andrea, W. J., Miller, G. H., and Sepúlveda, J. (2020). Lipid biomarkers quantify Holocene summer temperature and ice cap sensitivity in Icelandic lakes. Geophysical Research Letters, 47(3), e2019GL085728.

Hopmans, E.C., Schouten, S., Sinninghe Damsté, J.S., 2016. The effect of improved chromatography on GDGT-based palaeoproxies. Organic Geochemistry 93, 1–6.

Horne, A.J., Goldman, C.R., 1994. Limnology, Vol. 2. McGraw-Hill, New York.

Huguet, C., Hopmans, E.C., Febo-Ayala, W., Thompson, D.H., Sinninghe Damsté, J.S., Schouten, S., 2006. An improved method to determine the absolute abundance of glycerol dibiphytanyl glycerol tetraether lipids. Organic Geochemistry 37, 1036–1041.

James, C., Fisher, J., Russell, V., Collings, S., Moss, B., 2005. Nitrate availability and hydrophyte species richness in shallow lakes. Freshwater Biology 50, 1049–1063.

Kirkels, F.M., Zwart, H.M., Usman, M.O., Hou, S., Ponton, C., Giosan, L., Eglinton, T.I., Peterse, F., 2022. From soil to sea: sources and transport of organic carbon traced by tetraether lipids in the monsoonal Godavari River. India. Biogeosciences 19, 3979–4010.

Kunzmann, A.J., Ehret, H., Yohannes, E., Straile, D., Rothhaupt, K.O., 2019. Calanoid copepod grazing affects plankton size structure and composition in a deep, large lake. Journal of Plankton Research 41, 955–966.

Lever, M.A., Torti, A., Eickenbusch, P., Michaud, A.B., Šantl-Temkiv, T., Jørgensen, B.B., 2015. A modular method for the extraction of DNA and RNA, and the separation of DNA pools from diverse environmental sample types. Frontiers in Microbiology 6, 476.

Lliros, M., Inceoğlu, Ö., García-Armisen, T., Anzil, A., Leporcq, B., Pigneur, L.M., Viroux, L., Darchambeau, F., Descy, J., Servais, P., 2014. Bacterial community composition in three freshwater reservoirs of different alkalinity and trophic status. PLoS One1 9, e116145.

Loomis, S.E., Russell, J.M., Heureux, A.M., D'Andrea, W.J., Sinninghe Damsté, J.S., 2014. Seasonal variability of branched glycerol dialkyl glycerol tetraethers (brGDGTs) in a temperate lake system. Geochimica et Cosmochimica Acta 144, 173–187.

Marcott, S.A., Shakun, J.D., 2015. Holocene climate change and its context for the future. Past Global Climate Changes Magazine. 23, 28–29.

Martínez-Sosa, P., Tierney, J.E., 2019. Lacustrine brGDGT response to microcosm and mesocosm incubations. Organic Geochemistry 127, 12–22.

Martínez-Sosa, P., Tierney, J.E., Meredith, L.K., 2020. Controlled lacustrine microcosms show a brGDGT response to environmental perturbations. Organic Geochemistry 145, 104041.

Martínez-Sosa, P., Tierney, J.E., Stefanescu, I.C., Crampton-Flood, E.D., Shuman, B.N., Routson, C., 2021. A global Bayesian temperature calibration for lacustrine brGDGTs. Geochimica et Cosmochimica Acta 305, 87–105.

McMurdie, P.J., Holmes, S., 2013. phyloseq: an R package for reproducible interactive analysis and graphics of microbiome census data. PLoS One1 8, e61217.

Miller, D.R., Habicht, M.H., Keisling, B.A., Castañeda, I.S., Bradley, R.S., 2018. A 900-year New England temperature reconstruction from in situ seasonally produced branched glycerol dialkyl glycerol tetraethers (brGDGTs). Climate of the Past 14, 1653–1667.

Naafs, B.D.A., Inglis, G.N., Zheng, Y., Amesbury, M.J., Biester, H., Bindler, R., Blewett, J., Burrows, M.A., del Castillo, T., Chambers, F.M., Cohen, A.D., Evershed, R.P., Feakins, S.J., Galka, M., Gallego-Sala, A., Gandois, L., Gray, D.M., Hatcher, P.G., Honorio Coronado, E.N., Hughes, P.D.M., Pancost, R.D., 2017. Introducing global peat-specific temperature and pH calibrations based on brGDGT bacterial lipids. Geochimica et Cosmochimica Acta 208, 285–301.

Naafs, B.D.A., Oliveira, A.S.F., Mulholland, A.J., 2021. Molecular dynamics simulations support the hypothesis that the brGDGT paleothermometer is based on homeoviscous adaptation. Geochimica et Cosmochimica Acta 312, 44–56.

Naeher, S., Peterse, F., Smittenberg, R.H., Niemann, H., Zigah, P.K., Schubert, C.J., 2014. Sources of glycerol dialkyl glycerol tetraethers (GDGTs) in catchment soils, water column and sediments of Lake Rotsee (Switzerland)–Implications for the application of GDGT-based proxies for lakes. Organic Geochemistry 66, 164–173.

Oksanen, J., Blanchet, F. G., Kindt, R., Legendre, P., Minchin, P. R., O'hara, R. B., Simpson, G. L., Solymos [aut], P., Steven, M. H. H., Szoecs, E., Wagner, H., Barbour, M., Bedward, M., Bolker, B., Borcard, D., Carvalho, G., Chirico, M., De Caceres, M., Evangelista, D. S. H., Oksanen, M. J. (2013). Package 'vegan'. Community ecology package, version, 2(9), 1-295.

Peterse, F., Kim, J.H., Schouten, S., Kristensen, D.K., Koç, N., Sinninghe Damsté, J.S., 2009. Constraints on the application of the MBT/CBT palaeothermometer at high latitude environments (Svalbard, Norway). Organic Geochemistry 40, 692–699.

Pomeroy, L.R., Sheldon, J.E., Sheldon Jr, W.M., 1994. Changes in bacterial numbers and leucine assimilation during estimations of microbial respiratory rates in seawater by the precision Winkler method. Applied and Environmental Microbiology 60, 328–332.

Raberg, J.H., Harning, D.J., Crump, S.E., de Wet, G., Blumm, A., Kopf, S., Geirsdóttir, Á., Miller, G.H., Sepúlveda, J., 2021. Revised fractional abundances and warm-season temperatures substantially improve brGDGT calibrations in lake sediments. Biogeosciences 18, 3579–3603.

Rogora, M., Mosello, R., Kamburska, L., Salmaso, N., Cerasino, L., Leoni, B., Garibaldi, L., Soler, V., Lepori, F., Colombo, L., Buzzi, F., 2015. Recent trends in chloride and sodium concentrations in the deep subalpine lakes (Northern Italy). Environmental Science and Pollution Research 22, 19013–19026.

Russell, J.M., Hopmans, E.C., Loomis, S.E., Liang, J., Sinninghe Damsté, J.S., 2018. Distributions of 5-and 6-methyl branched glycerol dialkyl glycerol tetraethers (brGDGTs) in East African lake sediment: Effects of temperature, pH, and new lacustrine paleotemperature calibrations. Organic Geochemistry 117, 56–69.

Sahonero-Canavesi, D.X., Siliakus, M.F., Abdala Asbun, A., Koenen, M., von Meijenfeldt, F.B., Boeren, S., Bale, N.J., Engelman, J.C., Fiege, C., Strack van Schijndel, L., Sinninghe Damsté, J.S., Villanueva, L., 2022. Disentangling the lipid divide: Identification of key enzymes for the biosynthesis of membrane-spanning and ether lipids in Bacteria. Science Advances 8, eabq8652.

Schouten, S., Hopmans, E.C., Pancost, R.D., Sinninghe Damsté, J.S., 2000. Widespread occurrence of structurally diverse tetraether membrane lipids: evidence for the ubiquitous presence of low-temperature relatives of hyperthermophiles. Proceedings of the National Academy of Sciences 97, 14421–14426.

Schouten, S., Hopmans, E.C., Sinninghe Damsté, J.S., 2013. The organic geochemistry of glycerol dialkyl glycerol tetraether lipids: A review. Organic Geochemistry 54, 19–61.

Schubert, C.J., Lucas, F.S., Durisch-Kaiser, E., Stierli, R., Diem, T., Scheidegger, O., Vazquez, F., Müller, B., 2010. Oxidation and emission of methane in a monomictic lake (Rotsee, Switzerland). Aquatic Sciences 72, 455–466.

Schwab, M.S., Gies, H., Freymond, C.V., Lupker, M., Haghipour, N., Eglinton, T.I., 2022. Environmental and hydrologic controls on sediment and organic carbon export from a subalpine catchment: insights from a time series. Biogeosciences 19, 5591–5616.

Shade, A., Kent, A.D., Jones, S.E., Newton, R.J., Triplett, E.W., McMahon, K.D., 2007. Interannual dynamics and phenology of bacterial communities in a eutrophic lake. Limnology and Oceanography 52, 487–494.

Shanahan, T.M., Hughen, K.A., Van Mooy, B.A., 2013. Temperature sensitivity of branched and isoprenoid GDGTs in Arctic lakes. Organic Geochemistry 64, 119–128.

Sinninghe Damsté, J.S., Hopmans, E.C., Pancost, R.D., Schouten, S., Geenevasen, J.A., 2000. Newly discovered non-isoprenoid glycerol dialkyl glycerol tetraether lipids in sediments. Chemical Communications 17, 1683–1684.

Sinninghe Damsté, J.S., Rijpstra, W.I.C., Hopmans, E.C., Foesel, B.U., Huber, K.J., Overmann, J., Nakagawa, S., Kim, J.M., Dunfield, P.F., Dadysh, S.N., Villanueva, L., 2018. An overview of the occurrence of ether-and ester-linked iso-diabolic acid membrane lipids in microbial cultures of the Acidobacteria: Implications for brGDGT paleoproxies for temperature and pH. Organic Geochemistry 124, 63–76.

Sinninghe Damsté, J.S., Rijpstra, W.I.C., Hopmans, E.C., Weijers, J.W., Foesel, B.U., Overmann, J., Dedysh, S.N., 2011. 13, 16-Dimethyl octacosanedioic acid (iso-diabolic acid), a common membrane-spanning lipid of Acidobacteria subdivisions 1 and 3. Applied and Environmental Microbiology 77, 4147–4154.

Sinninghe Damsté, J.S., Rijpstra, W.I.C., Hopmans, E.C., Foesel, B.U., Wüst, P.K., Overmann, J., Tank, M., Bryant, D.A., Dunfield, P.F., Houghton, K., Stott, M.B., 2014. Ether-and ester-bound iso-diabolic acid and other lipids in members of Acidobacteria subdivision 4. Applied and Environmental Microbiology 80, 5207–5218.

Smith, V.H., Tilman, G.D., Nekola, J.C., 1999. Eutrophication: impacts of excess nutrient inputs on freshwater, marine, and terrestrial ecosystems. Environmental Pollution 100, 179–196.

Stefanescu, I.C., Shuman, B.N., Tierney, J.E., 2021. Temperature and water depth effects on brGDGT distributions in sub-alpine lakes of mid-latitude North America. Organic Geochemistry 152, 104174.

Su, Y., Lammers, M., Zhang, Y., van Bree, L., Liu, Z., Reichart, G.J., Middelburg, J.J., 2017. Sources of organic matter for bacteria in sediments of Lake Rotsee, Switzerland. Journal of Paleolimnology 58, 391–402.

Tierney, J.E., Poulsen, C.J., Montañez, I.P., Bhattacharya, T., Feng, R., Ford, H.L., Hönisch, B., Inglis, G.N., Petersen, S.V., Sagoo, N., Tabor, C.R., Thirumalai, K., Zhu, J., Burls, N.J., Foster, G.L., Godderis, Y., Huber, B.T., Ivany, L.C., Turner, S.K., Lunt, D.J., Mcelwain, J.C., Mills, B.J.W., Otto-Bliesner, B.L., Ridgewell, A., Zhang, Y. G., 2020. Past climates inform our future. Science 370 (6517), eaay3701.

Tierney, J.E., Russell, J.M., 2009. Distributions of branched GDGTs in a tropical lake system: implications for lacustrine application of the MBT/CBT paleoproxy. Organic Geochemistry 40, 1032–1036.

Tierney, J.E., Russell, J.M., Eggermont, H., Hopmans, E.C., Verschuren, D., Sinninghe Damsté, J.S., 2010. Environmental controls on branched tetraether lipid distributions in tropical East African lake sediments. Geochimica et Cosmochimica Acta 74, 4902–4918.

Van Bree, L., Peterse, F., Baxter, A.J., De Crop, W., Van Grinsven, S., Villanueva, L., Verschren, D., Sinninghe Damsté, J.S., 2020. Seasonal variability and sources of in situ brGDGT production in a permanently stratified African crater lake. Biogeosciences 17, 5443–5463.

Wang, H., Liu, W., He, Y., Zhou, A., Zhao, H., Liu, H., Cao, Y., Hu, J., Meng, B., Jiang, J., Kolpakova, M., Krivonogov, S., Liu, Z., 2021. Salinity-controlled isomerization of lacustrine brGDGTs impacts the associated MBT5ME'terrestrial temperature index. Geochimica et Cosmochimica Acta 305, 33–48.

Weber, Y., Sinninghe Damsté, J.S., Hopmans, E.C., Lehmann, M.F., Niemann, H., 2017. Incomplete recovery of intact polar glycerol dialkyl glycerol tetraethers from lacustrine suspended biomass. Limnology and Oceanography: Methods 15, 782–793.

Weber, Y., Sinninghe Damsté, J.S., Zopfi, J., De Jonge, C., Gilli, A., Schubert, C.J., Lepori, L., Lehmann, M.F., Niemann, H., 2018. Redox-dependent niche differentiation provides evidence for multiple bacterial sources of glycerol tetraether lipids in lakes. Proceedings of the National Academy of Sciences 115, 10926–10931.

Weijers, J.W., Schouten, S., Spaargaren, O.C., Sinninghe Damsté, J.S., 2006. Occurrence and distribution of tetraether membrane lipids in soils: Implications for the use of the TEX86 proxy and the BIT index. Organic Geochemistry 37, 1680–1693.

Weijers, J.W., Schouten, S., van den Donker, J.C., Hopmans, E.C., Sinninghe Damsté, J. S., 2007. Environmental controls on bacterial tetraether membrane lipid distribution in soils. Geochimica et Cosmochimica Acta 71, 703–713.

Weijers, J.W., Panoto, E., van Bleijswijk, J., Schouten, S., Rijpstra, W.I.C., Balk, M., Stams, A.J.M., Sinninghe Damsté, J.S., 2009. Constraints on the biological source (s) of the orphan branched tetraether membrane lipids. Geomicrobiology Journal 26, 402–414.

Weyhenmeyer, G.A., Hartmann, J., Hessen, D.O., Kopáček, J., Hejzlar, J., Jacquet, S., Hamilton, S.K., Verburg, P., Leach, T.H., Schmid, M., Flaim, G., Nõges, T., Nõges, P., Wentzky, V.C., Rogora, M., Rusak, J.A., Kosten, S., Paterson, A.M., Teubner, K., Higgins, S.N., Lawrence, G., Kangur, K., Kokorite, I., Cerasino, L., Funk, L., Harvey, R., Moatar, F., deWit, H.A., Zechmeister, T., 2019. Widespread diminishing anthropogenic effects on calcium in freshwaters. Science Reports 9, 1–10.

White, P.A., Kalff, J., Rasmussen, J.B., Gasol, J.M., 1991. The Effect of Temperature and Algal Biomass on Bacterial Production and Specific Growth Rate in Freshwater and Marine Habitats. Microbial Ecology 21, 99–118.

Xiao, W., Wang, Y., Zhou, S., Hu, L., Yang, H., Xu, Y., 2016. Ubiquitous production of branched glycerol dialkyl glycerol tetraethers (brGDGTs) in global marine environments: a new source indicator for brGDGTs. Biogeosciences 13, 5883–5894.

Yamamoto, M., Shimamoto, A., Fukuhara, T., Tanaka, Y., 2016. Source, settling and degradation of branched glycerol dialkyl glycerol tetraethers in the marine water column. Geochimica et Cosmochimica Acta 191, 239–254.

Zak, D., Hupfer, M., Cabezas, A., Jurasinski, G., Audet, J., Kleeberg, A., McInnes, R., Kristiansen, S.M., Petersen, R.J., Liu, H., Goldhammer, T., 2021. Sulphate in freshwater ecosystems: A review of sources, biogeochemical cycles, ecotoxicological effects and bioremediation. Earth-Science Reviews 212, 103446.

Zang, J., Lei, Y., Yang, H., 2018. Distribution of glycerol ethers in Turpan soils: implications for use of GDGT-based proxies in hot and dry regions. Frontiers of Earth Science 12, 862–876.

Zell, C., Kim, J.H., Hollander, D., Lorenzoni, L., Baker, P., Silva, C.G., Nittouer, C., Sinninghe Damsté, J.S., 2014. Sources and distributions of branched and isoprenoid tetraether lipids on the Amazon shelf and fan: Implications for the use of GDGT-based proxies in marine sediments. Geochimica et Cosmochimica Acta 139, 293–312.

Zeng, Z., Chen, H., Yang, H., Chen, Y., Yang, W., Feng, X., Pei., H, and Welander, P. V., 2022. Identification of a protein responsible for the synthesis of archaeal membrane-spanning GDGT lipids. Nature Communications 13, 1545.